CALCULATION OF CARRIERS IN DEPLETION REGION OF SEMICONDUCTORS WITH CAPACITANCE-VOLTAGE MEASUREMENTS

THESIS

Jong Hyun Kim
Captain, ROKA

AFIT/GEO/ENP/88D-8

DEPARTMENT OF THE AIR FORCE
AIR UNIVERSITY
AIR FORCE INSTITUTE OF TECHNOLOGY

Wright-Patterson Air Force Base, Ohio

(1)

AFIT/GEO/ENP/88D-8

CALCULATION OF CARRIERS IN DEPLETION REGION OF SEMICONDUCTORS WITH CAPACITANCE-VOLTAGE MEASUREMENTS

THESIS

Jong Hyun Kim
Captain, ROKA

AFIT/GEO/ENP/88D-8

Approved for public release; distribution unlimited

AFIT/GEO/ENP/88D-8

CALCULATION OF CARRIERS IN DEPLETION REGION OF SEMICONDUCTORS WITH CAPACITANCE-VOLTAGE MEASUREMENTS

THESIS

Presented to the Faculty of the School of Engineering
of the Air Force Institute of Technology
Air University
In Partial Fulfillment of the
Requirements for the Degree of
Master of Science in Electro Optics

Jong Hyun Kim, B.S.
Captain, ROKA

December 1988

Acknowledgments

I dedicate this work to my parents, my senior officers and their family, and my friends. Without all of their help, none of this would have been possible.

Many individuals helped me to perform experiments and to write computer programs at the Avionics Laboratory. In particular, I would like to thank Mr. Edward Sturtz and Capt. David Elsaesser. I would also like to thank my thesis advisors, Dr. Y. K. Yeo and Dr. R. L. Hengehold. Their special combination of inspiration, knowledge, and humor made this work actually fun.

Jong Hyun Kim

Table of Contents

List of Figures

List of Tables

Abstract

Profiles obtained by the capacitance-voltage (C-V) method cannot give carrier distributions information right from the semiconductor surface. Since the prediction of ultimate device performance depends strongly upon an accurate knowledge of the entire carrier depth profile, it is very important to know this profile for the entire crystal including the surface depletion layer. A method was developed for obtaining carrier depth profiles within the initial depletion region of semiconductor from the measured C-V data. This method was successfully applied to simulated C–V profile data created from various known linear, parabolic, and LSS Gaussian distributions, and then finally was demonstrated through experimentally measured C-V profiles obtained from Si-implanted GaAs. In this method, barrier potential was assumed to be 0.8 eV for n-type Si-implanted GaAs.

CALCULATION OF CARRIERS IN DEPLETION REGION OF SEMICONDUCTORS WITH CAPACITANCE-VOLTAGE MEASUREMENTS

I. INTRODUCTION

The electrical and optical properties of semiconductors are altered significantly by adding appropriate impurities into the materials via doping. Characterization of these properties is very important in their application to electronic and opto-electronic devices such as field effect transistors, integrated circuits, and laser diodes. The electrical properties of semiconductors are usually carried out by Hall-effect/sheet-resistivity measurements and capacitance-voltage (C-V) profiling (7:645).

Both methods, however, have certain advantages as well as some limitations. One of the limitations of the C-V method is that it cannot give carrier distribution information within an initial depletion region near the semiconductor surface. Most of the time, the C-V method provide only a partial profile of the carrier distribution as shown in Figure 1. Thus, the whole profile is unknown and often times peak carrier concentration is also unknown. Even if it can give the peak carrier concentration, the entire carrier depth profile is very uncertain. Carrier concentration is an important parameter in electronic and opto-electronic device performance. Since the prediction of ultimate device performance depends strongly upon an accurate knowledge of the entire carrier depth profile, it is very important to know this profile for the entire crystal including the initial depletion layer. It is therefore essential to develop a method for determining the entire carrier deptn profile, right from the semiconductor surface, using the data obtained by a standard C-V depth profile measurement.

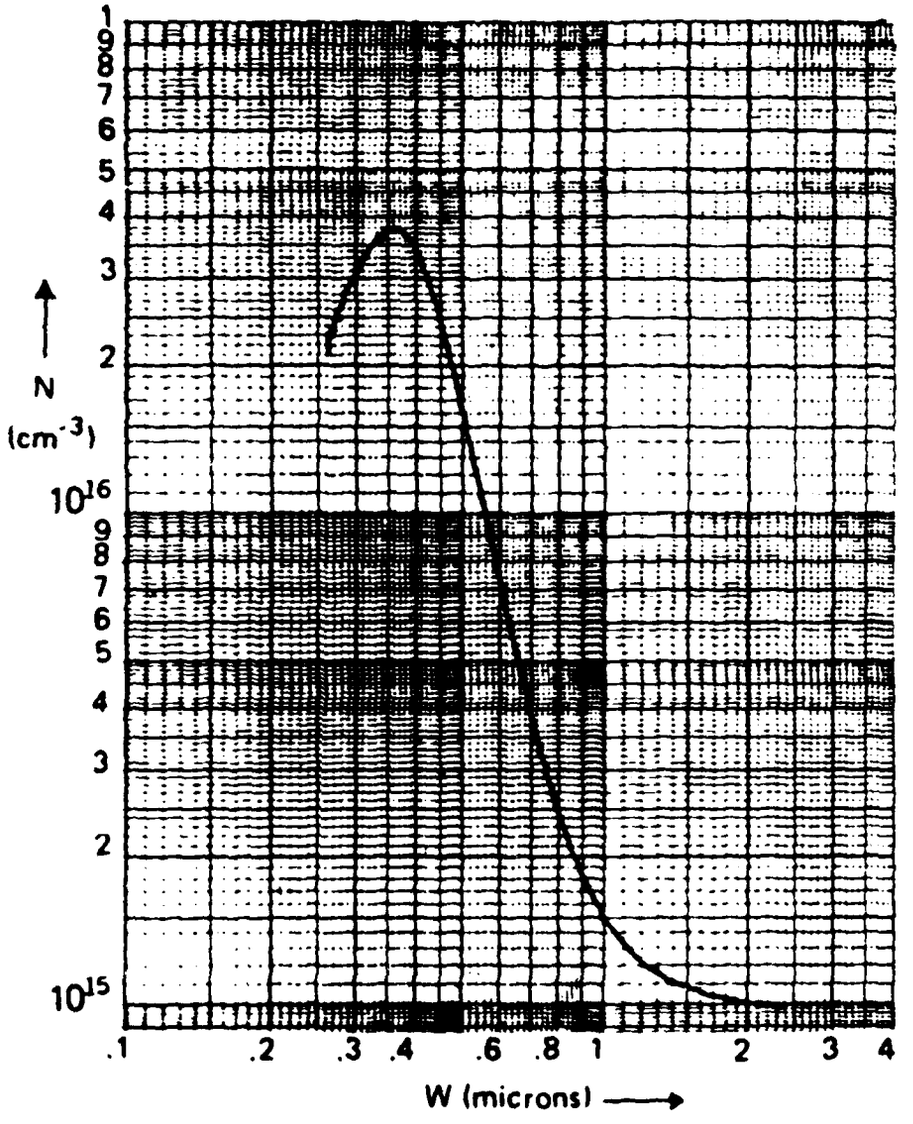

Figure 1. Ion Implanted Carrier Concentration Distribution by C–V method

1.1 Problem

How can a physicist calculate the carrier concentrations within the initial depletion region of semiconductor with C-V profile measurements and a chemical layer removal technique?

1.2 Summary of Current Knowledge

In recent years, the use of ion implantation as a means of introducing impurities into a semi-insulating semiconductor for the purpose of device fabrication has been given considerable attention. For example, active layers in microwave FETs (Field Effect Transistors) must be precisely controlled to depths of about 1 micron (3:14). This requirement is difficult to meet by standard techniques of epitaxial growth or thermal diffusion. However, ion implantation allows one to control the doping profile by simply varying the energy and fluence of the incident ions. Thus, theoretically, a continuous variation of the fluence and energy of the incident ions can produce any desired dopant distribution (1:9). In addition, ion implantation can produce good uniformity of implants over large regions, as well as reproducibility from wafer to wafer (2:122).

Of particular interest is a silicon-implanted GaAs, since Si is a relatively light atom and is therefore readily accelerated, with modest energy requirements, to velocities necessary to produce useful implant depths. Furthermore, low dose implants of Si in GaAs have produced high electrical activation efficiencies, which are more difficult to achieve with other n-type dopants such as S and Se (18:27).

There are many other applications for ion implantation which show considerable promise. For example, in a research project conducted for NASA, Woo constructed complementary-metal-oxide-semiconductor/silicon-on-sapphire circuits (CMOS/SOS) by ion implantation which were one third faster than those fabricated by diffusion (24). Other researchers have also demonstrated the feasibility of pro-

ducing electrically insulating layers in device materials by ion implantation, in lieu of the more common mesa techniques (3:17).

In general, for device applications, the carrier profiles of implanted semiconductors must be accurately measured. The two common electrical means for accomplishing this are capacitance-voltage (C-V) profiling and the differential Hall method. The differential Hall method can be used for both n-type and p-type materials. While C-V profiling makes use of static charge to determine the carrier profile, Hall measurements use only the mobile carriers. Sheet-carrier concentrations and average mobilities of thin epitaxial or ion-implanted layers of semiconductors are usually obtained by the Hall-effect/sheet-resistivity measurement method. Also, carrier and mobility depth profiles of these layers are often obtained through the combined use of the chemical-layer-removal technique and the Hall-effect/sheet-resistivity method (4:5070). Hall-effect and sheet resistivity measurements were made using the standard van der Pauw technique (25:6). This technique is characterized by measuring the sheet carrier concentration in carriers $/cm^2$, which corresponds to the total number of electrically active carriers below the surface per unit surface area. Then, a thin layer is removed by chemical etching. Another Hall-effect measurement can be used to find the carrier concentration in the removed layer. A subsequent measurement of the sheet carrier concentration reveals the density of activated ions in the layer which has been etched. An obvious disadvantage with this technique is that it is destructive, and therefore, measurements may not be repeated. Another problem with differential Hall profiling is that a surface depletion region produced by the filling of accepter-type surface electronic states results in the measurement of profile. Because of the surface depletion effect, the true profile is not only shifted but also contracted. This translation is due to the fact that Hall measurements make use of only mobile carriers, since only the carriers past the edge of the depletion width are measured. Furthermore, the distortion occurs because the depletion widths are a function of carrier concentration, which, of course, varies with depth. Small depletion widths

occur where the concentration of implanted ions is large and large depletion widths where the concentration is small. However, a surface depletion correction can be made to the measured apparent Hall profiles (4: 5070-5075).

The C-V method uses a reversed biased Shottky (14) barrier on the semiconductor to create a variable depletion width which can be found from its capacitance. As the reverse bias is increased, the depletion width extends deeper into the material, decreasing the capacitance and uncovering more dopant ions. The density of carriers at the edge of the depletion width is thus related to the differential change of capacitance with bias voltage. With the advent of ion implantation for semiconductor device fabrication, the determination of the ion-implanted impurity atom distribution in semiconductor material is important both in fundamental investigations and in such practical applications as the design and development of semiconductor devices. For example, in RF power transistors, junctions 0.1 μ apart are required. For shallow junctions, the method frequently used to determine the ion-implanted profiles is the differential capacitance technique. Other methods, such as the two-point probe spreading resistance technique, do not have the spatial resolution required by shallow ion-implanted profiles. The C-V method is nondestructive. It provides ease of measurements and adaptability to automation and it measures electrically active impurity concentrations. However, the C-V method does not give a profile within the initial depletion width at zero bias voltage, and this depletion width is often as large as 0.2 μm. Also, the C-V method can be practically applied only to n-type materials (21: 319-328).

1.3 Scope

This research is to develop a method of calculating the carrier concentrations within the initial depletion region of semiconductors by combining the C-V measurements and a chemical layer removal technique.

The method was tested on simulated C–V profile data and experimental C–

V data of Si-implanted GaAs. The GaAs samples used were <100> oriented and usually Cr-doped during crystal growth. The samples were ion implanted at room temperature at an ion energy of 100 or 200 keV. The ion dose was 8×10^{12} or 1×10^{13} cm^{-2}. The samples were annealed at either 800 or 850 °C for 15 minutes.

1.4 Methodology

The approach was divided into three phases. The preliminary research phase consisted of a familiarization with the ion implantation process. Learning the properties and limitations of ion implantation was essential for understanding a doping.

The second phase reviewed the theoretical basis of the C-V method, the cause of the initial depletion region, the chemical layer removal technique, semiconductor crystals, Poisson's equation, and computer programs developed to analyze and implement the calculation method.

In the development phase, simulated C-V profile data was created from various known carrier profiles, and a method of calculating carriers in the depletion region was developed from the known data. After that, the C-V measurements were carried out, and the developed computational analysis method was applied to the obtained experimental data.

1.5 Materials and Equipment

The material used was <100> oriented undoped semi-insulating GaAs. The research itself also required a computer, software packages, the Hewlett-Packard Model 4061 Semiconductor/Component Test System, PN 4200 Polaron's Semiconductor Profiler and the Hewlett-Packard Model 86B Computer. The software needed to be able to handle the carrier concentrations within the initial depletion region and run various mathematical programs.

1.6 Other Support

In addition, completion of this research required assistance from the Avionics Laboratory during its early stages. The required characterization equipment was available at the Electronic Research Branch of the Avionics Laboratory, and the measurements were done at that facility.

1.7 Sequence of Presentation

Chapter II provides background information on ion-implantation and ion range statistics. *Chapter II* also reviews the theoretical basis of the C-V method and the source of the initial depletion region. *Chapter III* describes the Si-implanted GaAs sample preparation and C-V measurements. *Chapter IV* discusses the theory of the method developed for finding the depletion region concentrations, starting with Poisson's equation. *Chapter V* describes the computer programs developed to analyze and implement the methods. *Chapter VI* shows and discusses the performance of the methods. *Chapter VII* presents the conclusions of this study.

II. BACKGROUND

2.1 Ion Implantation

By introducing certain impurities into a semiconductor, the electrical and optical properties of the semiconductor may be changed. This process is called doping, and may be employed during the crystal growth process, or by diffusion or ion implantation in the post growth process. The creation of a semi-insulating GaAs substrate involves chromium doping during the crystal growth process to electrically compensate for impurities in the substrate. Conventionally, the thermal diffusion technique is used to uniformly dope large crystal surfaces.

Research into ion implantation for the doping of silicon to produce specialized devices increased rapidly in the United States and Europe after 1965. The abrupt nature of the ion implanted junction has been used to fabricate avalanche photodetectors, IMPATT (Impact ionization Avalanche Transit Time) diodes and a shallow junction having the approximate characteristics of a Schottky diode. The precise control of the depth profile offered by ion implantation has been used to make the narrow base regions in microwave planar p-n-p and n-p-n transistors. Varactor diodes, which incorporate a number of integrated profiles, have also been created using ion implantation.

The most striking application of ion implantation in device technology has been in the automatic alignment of the gate electrode of a metal oxide silicon transistor to the source and drain regions. The technique was first described by Bower and Bill (1966). Shannon, Stephen, and Freeman (1969) have given the details of a MOST (Metal Oxide Semiconductor Transistor) with a cut-off frequency of 1.8 GHz and have stressed the importance of applying ion implantation to MOS (Metal Oxide Semiconductor) arrays. Glotin et al. (1967) have given details of similar work in France, while Burt (1969) has described the application of implantation to an MOS tetrode structure (1:478).

The ion implantation doping technique involves the injection of the dopants into the substrate using an energetic ion beam and offers certain advantages over the other two doping techniques. For example, ion implantation allows accurate control of the dopant concentration, well defined dopant profiles, good reproducibility, slight lateral spreading of the dopant, selective area doping, good uniformity over a relatively large area, selective area implantation, planar type device technology, and high yield at low cost production of semiconductors. In addition, ion implantation is especially useful for the doping of compound semiconductors at relatively low temperatures.

Despite the many advantages of ion implantation, the technique does have problems. The bombardment of the dopants into the substrate using an energetic ion beam results in such undesirable crystalline defects as vacancies, interstitials, and an amorphous like lattice (1:162). Since some of the implanted ions do not go into substitutional lattice sites, all of the ions do not become electrically active. Thermal annealing is required to reorder the crystal, and increase electrical activity of the ion implants. However, at the high temperatures required for crystal annealing (800-1000°C), the dopant and substrate elements will diffuse to the surface of the crystal. To prevent the loss of these ions, a surface cap called an encapsulant is used during the high temperature annealing process.

2.2 Lindhard, Sharff, and Schiott (LSS) Theory

The LSS theory describes the distribution of implanted ions with depth in an amorphous solid. When an energetic ion enters a solid, it loses energy to either the target-atom's nuclei or electrons through collisions, and is deflected from its original trajectory until finally brought to rest. If the target material is amorphous, the stopping process for any particular ion of an incident monoenergetic beam will be random, and the distribution of implanted ions will be approximately Gaussian, characterized by an average projected range and a standard deviation (6:44).

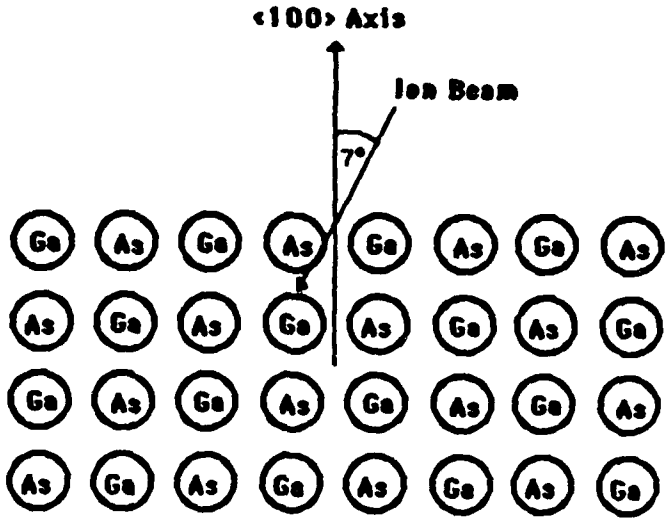

Figure 2. Ion Beam Orientation to Prevent "Channeling"

In crystalline targets, the distribution of implanted ions is dependent on the orientation of the substrate during the implantation. If the incident beam is aligned with one of the major crystal axes or planes, then channeling may take place. This phenomenon is characterized by some of the implanted ions penetrating to depths far greater than predicted for amorphous targets. This problem can generally be minimized by misaligning the target crystal. The ion beam is then incident in a nonchanneling direction, making the target material appear amorphous (2,6). Figure 2 shows the ion beam orientation necessary to prevent channeling.

The LSS theory considers the effect of the stopping power of the atoms in the substrate on the implanted ions through various kinetic energy loss mechanisms. The result is a Gaussian distribution in which the average projected range, R_p, and the standard deviation of the position of the peak of the distribution, σ_p, depend upon the energy, as well as the atomic number of the implanted ions and that of the substrate. Gibbons et al (5) have developed a computer program to calculate R_p and σ_p and have tabulated the results for various energies, implanted ions, and

GAUSSIAN APPROXIMATION OF IMPURITY CONCENTRATION, $N(X_P)$:

$$N(X_P) = \frac{\phi}{\sigma_P\sqrt{2\pi}} \exp\left[-\frac{(X_P - R_P)^2}{2\sigma_P^2}\right],$$

WHERE ϕ IS ION DOSE/CM^2, AND X_P IS A MEASURED DISTANCE ALONG THE DIRECTION OF INCIDENT ION BEAM.

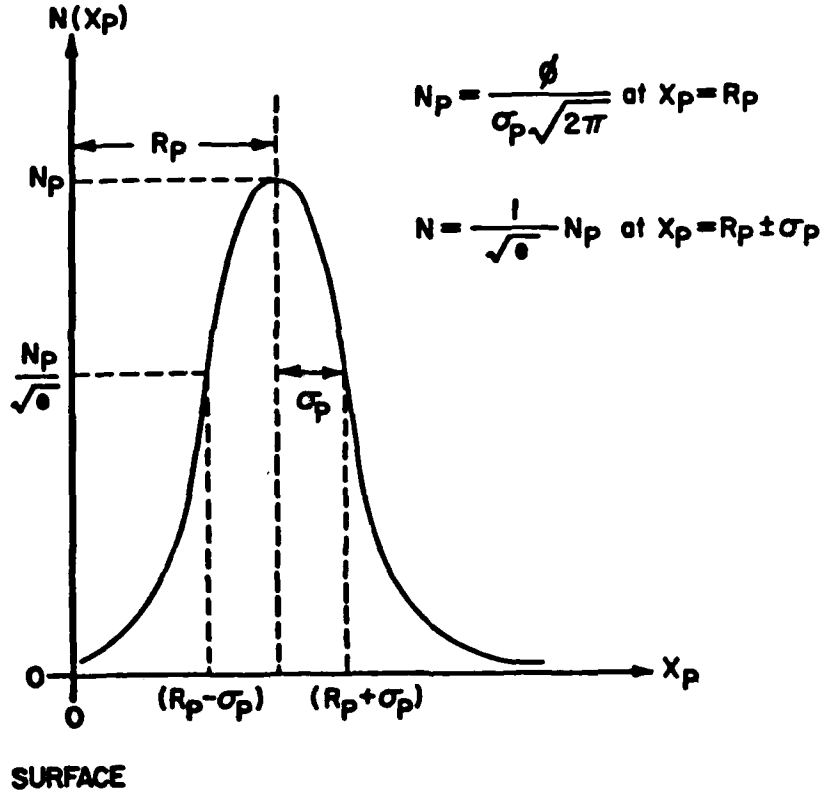

Figure 3. LSS Theoretical Ion Depth Profile

substrates. For example, Si ions with an energy of 100keV have a projected range in GaAs of 0.085 μm and a standard deviation of 0.0442 μm.

Lindhard, Sharff, and Schiott used the Thomas-Fermi interatomic potential to calculate the ion energy loss due to nuclear collisions and the range or depth that ions would go below the surface of the substrate. Assuming a Gaussian range distribution, they also calculated a mean square fluctuation in this range (1:36-39). The ion implanted dopant concentration is then given by

$$N(x_p) = \frac{\phi}{\sigma_p\sqrt{2\pi}} EXP[\frac{-(x_p - R_p)^2}{2\sigma_p^2}] \qquad (1)$$

where N(x_p) is the dopant concentration at a depth x_p measured from the surface, ϕ is the ion beam fluence, and σ_p is the standard deviation in the projected range R_p. Figure 3 provides a theoretical LSS ion depth profile.

2.3 Depletion Region of Metal-Semiconductor Contacts

When two metals having different work functions are brought into contact with one another, a brief transient current flow will transfer electrons from the metal with the larger Fermi energy to the one with the smaller Fermi energy. An equilibrium contact potential difference will therefore be generated between the two metals. The semiconductor differs from a metallic substance, however, in that an electric field may exist within the interior of a semiconductor. For this reason, the contact potential drop between the metal and semiconductor may take place within the semiconductor rather than at the contact interface. In the simplest possible instance, what may happen is illustrated in Figures 4 and 5 for the case of contact between a metal and an n-type semiconductor crystal, where the work function of the metal, ϕ_M, is larger than the work function ϕ_S associated with the semiconductor. The field which arises due to the contact potential difference exists now largely within the semiconductor. The potential energy of an electron at rest at the bottem of the conduction band in the interior of the crystal thus differs from the potential energy of such an electron at the surface by the amount e($\phi_M - \phi_S$). As a result, the conduction and valence band

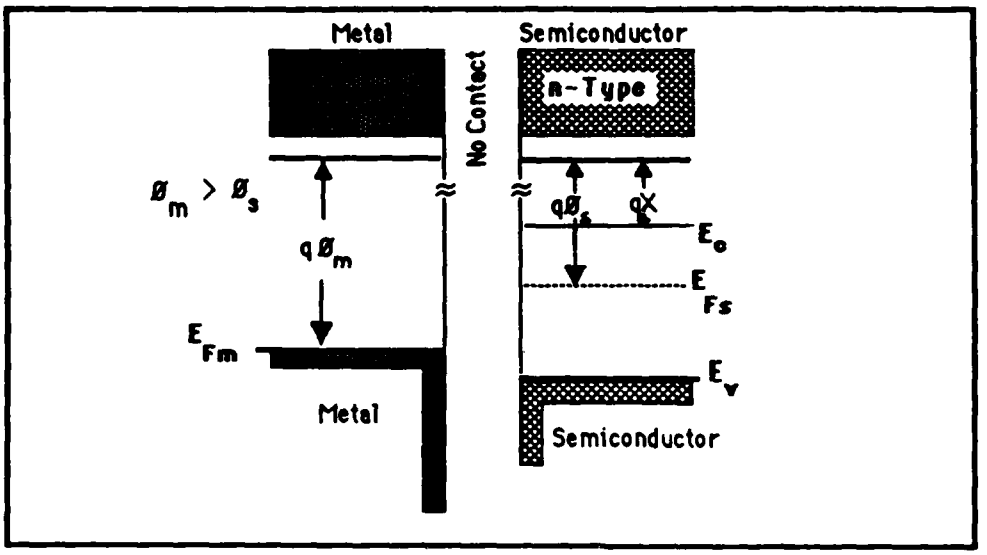

Figure 4. Energy Band Diagram for a Metal-Semiconductor Contact Before Joining

edges are shifted with respect to the Fermi level as shown in Figure 5. The positive space charge density in the surface region, due to the excess concentration of ionized donor atoms over the electron population is enough to produce a field sufficient to sustain the potential difference $\phi_M - \phi_S$ between the two materials (10:478).

When a metal is brought into contact with an n-type semiconductor, the Fermi energy level E_F stays constant across the metal-semiconductor boundary as shown in the energy-band diagram of Figure 5. The conduction band minimum E_C of the semiconductor starts out level at a distance W from the metal and then rises to a barrier height $q\phi_B$ at the metal surface, where q is the electronic charge and ϕ_B is the barrier potential. The built-in potential V_{bi} is the difference between the potential at the metal surface and the potential at W, which is called the depletion width. Chandra et al. (7:646) showed that the difference between the conduction

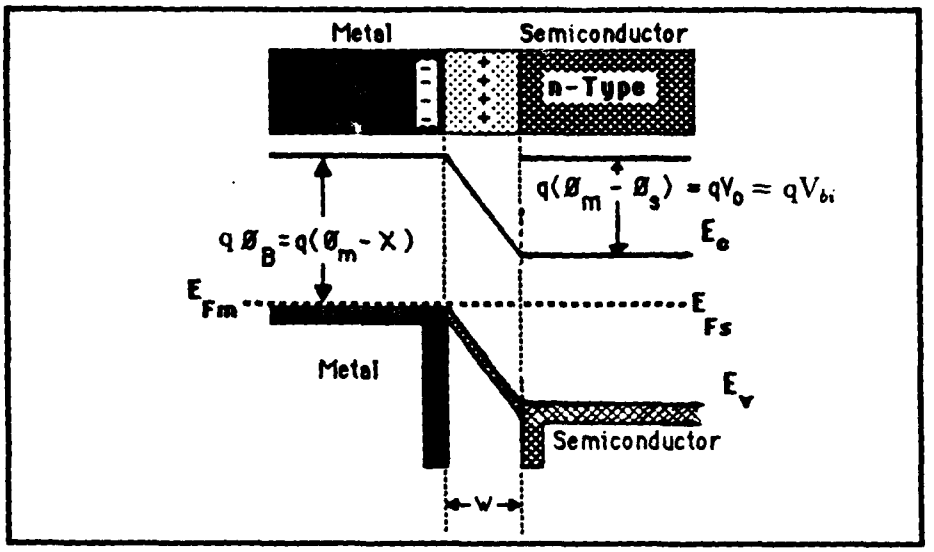

Figure 5. Depletion Region Due to Schottky Barrier with Zero Bias

band minimum and the Fermi level is given by

$$E_C - E_F = kT\ ln[N_C/N(W)], \tag{2}$$

where k is the Boltzmann constant, T is the temperature, N_C is the density of states at the conduction band minimum, and N(W) is the carrier concentration at the depletion width W. The carrier concentration N is

$$N = N_D - N_A - n + p, \tag{3}$$

where N_D is the donor impurity concentration, N_A is the acceptor concentration, n is the electron concentration, and p is the hole concentration. The electron and hole concentration are negligible where $N_D - N_A$ is high. The built-in potential is then

$$V_{bi} = \phi_B - (kT/q)\ ln[N_C/(N_D - N_A)]. \tag{4}$$

According to Schottky (14:4), the built-in potential V_{bi} should be the difference between the work functions of the metal and the semiconductor, $V_{bi} = \phi_M$ -

ϕ_S. However, experiments showed that the rectification of metal-semiconductor contacts can be independent of the metal work function. In 1947, Bardeen (9:5) showed that the surface barrier potential ϕ_B is determined by surface states. The surface states produce the potential even without a metal contact. When contact is made with a metal, the difference in work function between metal and semiconductor is compensated by surface state charge, rather than by a space charge as is ordinarily assumed, so that the space charge layer is independent of the metal. Rectification characteristics are then independent of the metal. The total strength of the double layer at a rectifying junction between a metal and semiconductor is fixed by the difference in chemical potentials, and so depends on the bulk properties of the metal and semiconductor, and is independent of the work functions of the surfaces before they are brought into contact. As explained by McKelvey (10:485), the Soviet physicist Tamm showed in 1932 that the surface states are caused by the ending of a periodic square-well potential, such as the Kronig-Penny crystal model, by a surface potential barrier, as shown in Figure 6 and 7. These additional states within the forbidden energy band of the Kronig-Penny model are the discrete allowed energy levels of wave functions localized near the surface. Shockley (11) calculated that there is one surface state for each surface atom. Surface states can also be created by impurity atoms, oxide layers, and surface imperfections. Treating the surface electronic states as unfilled oribitals or dangling bonds, Massies et al. (12:64) experimentally observed the electron transition of a Ga 3d orbital to a dangling Ga bond on the (100) face of GaAs.

The charging of the surface states causes the conduction band minimum and the valence band maximum to rise as they approach the surface. Henisch (13:184) explains that the Fermi energy level also rises to the surface, but when the semiconductor is brought to the metal, its Fermi energy level falls to equal the Fermi energy level of the metal. This creates an electric field between the metal and the semiconductor. If the density of surface states is large enough to take any additional

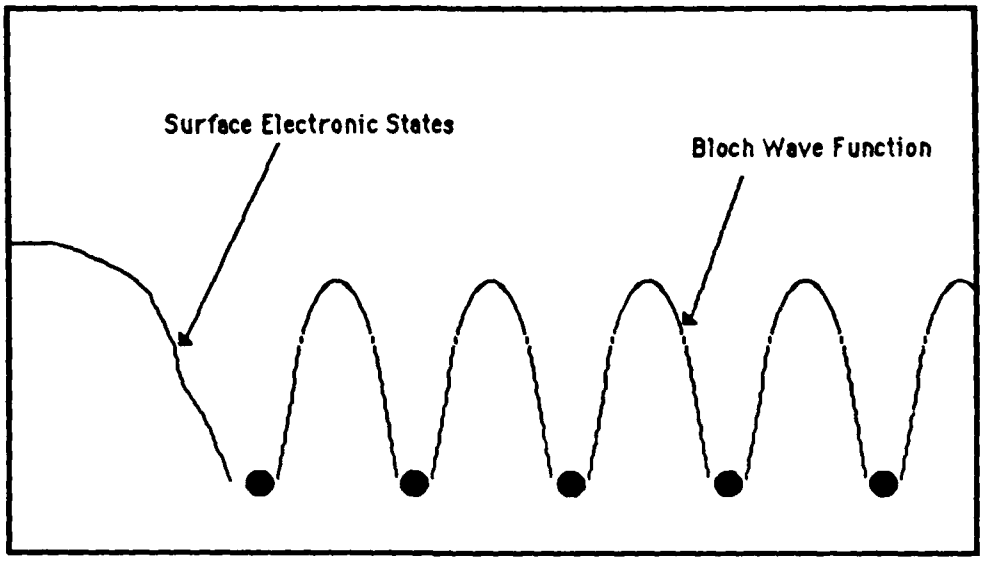

Figure 6. The Kronig-Penny Periodic Potential with Asymmetric Potential at the Crystal Surface

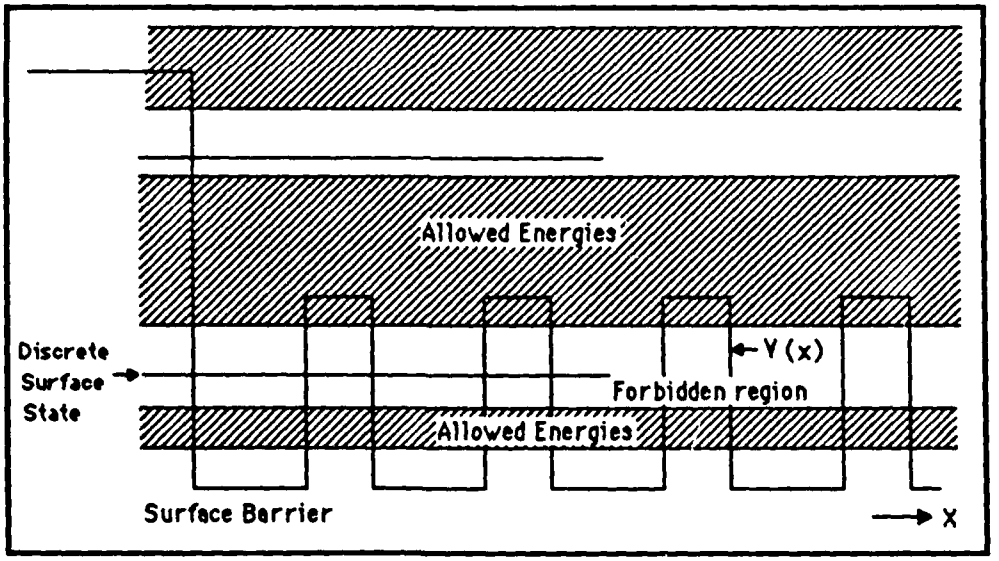

Figure 7. The Formation of Localized States in the Forbidden Energy Region at the Surface of a 1-D Crystal.

charges that would be caused by the electric field, without much changing the Fermi energy level, then the space charge in the semiconductor is unaffected by the metal contact, and the barrier height potential is independent of the metal work function (13:184).

2.4 Capacitance-Voltage Profiling

Doping profiles in semiconductors are commonly determined by a differential capacitance technique. A degenerately doped p-n junction or a metallic Schottky barrier is formed at the surface of the semiconductor. This junction is placed in reverse bias, and the capacitance of the transition layer is measured as a function of the bias voltage. Analysis of the capacitance versus bias voltage relationship is conveniently done using the depletion-layer approximation in which the semiconductor is assumed to be divided into a layer entirely depleted of charge carriers, and an interior region of perfect charge neutrality.

The theory behind using the C-V measurement as a profiling technique is based upon the validity of the so-called depletion approximation. This assumes that the depletion region consists entirely of the charge of the ionized acceptors and donors (immobile fixed impurities). Both kinds of mobil carriers are very small compared with the fixed impurity concentrations. It neglects the regions which are neither fully depleted nor approximately neutral. It assumes that the charge density in the depletion region is constant.

When a metal and an n-type semiconductor are brought together, a space charge or depletion region is formed as shown in Figure 5. When a reverse bias voltage is applied to the contact, more electrons leave the semiconductor to the metal, extending the depletion width x deeper into the semiconductor as shown in Figure 8. The space charge region can be treated as a voltage dependent parallel plate capacitor, with capacitance

$$C = \epsilon\epsilon_o A/x, \tag{5}$$

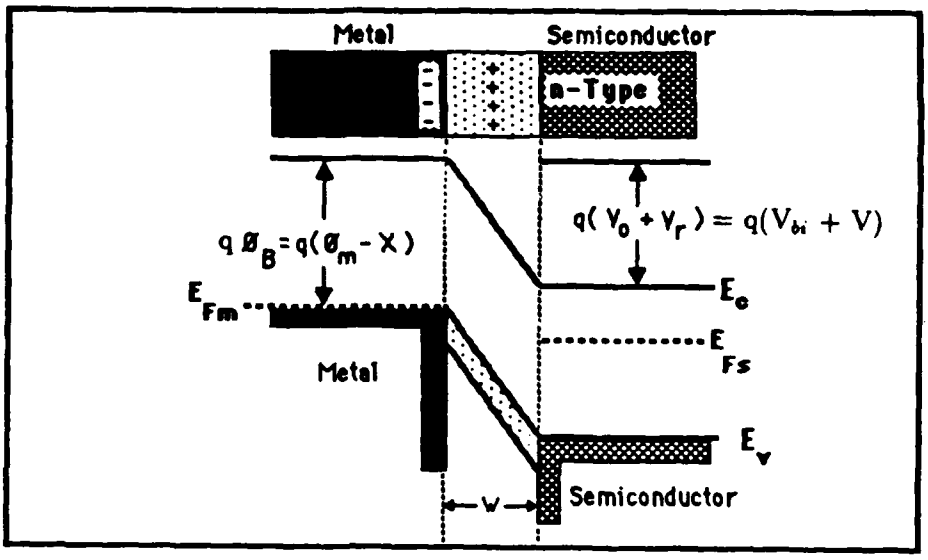

Figure 8. Depletion Region Due to a Metal-Semiconductor Contact with Applied Bias

where C is the capacitance in Farads, ϵ_o is the permittivity of free space in F/cm, ϵ is the relative dielectric constant, A is the area of the metal contact in cm^2, and x is the depletion width in cm. As the applied bias voltage V increases, x increases, and C decreases.

In 1942, Schottky had the idea of using capacitance measurements to obtain dopant profiles (14).

Copeland (15), Miller (16), and Nakhamanson (17) improved upon Schottky's idea to obtain the following equation for dopant profiles:

$$N(x) = \frac{-C^3}{\epsilon\epsilon_o q A^2 (dC/dV)} \quad at \quad x = \epsilon\epsilon_o A/C, \tag{6}$$

where N(x) is the carrier concentration at depth x below the semiconductor surface. The bias voltage is increased in small increments, and the capacitance is measured for each voltage to obtain dC/dV at each capacitance. This has been the basis of extensive use of the differential C-V measurement technique as a means of deter-

mining impurity profiles in semiconductors, especially the ion-implanted impurity profiles. There are three main reasons for its popularity. First, it measures the electrically active impurity concentration which is of primary importance in fabricating devices; second, it is nondestructive; and third, it provides ease of measurement and adaptability to automation.

To measure the capacitance, the bias voltages are actually superimposed upon an alternating voltage at frequency ω. The measured capacitance is

$$\acute{C} = C/(1 - \omega^2 r^2 C^2), \tag{7}$$

where C is the actual depletion layer capacitance, and r is a series resistance within the semiconductor (16:1106). The quantity ωrC is made small so that $\acute{C}$ is approximately C. This is done by reducing the metal contact area to reduce C, requiring r to be small in the semiconductor, and making ω as small as possible without ruining the signal-to-noise ratio. The frequency must also be kept high compared to the relaxation times of any traps present in the semiconductor (16:1106). Traps hold on to electrons much longer than most dopant atoms and distort the measured profile. The best frequency for GaAs is usually about 1MHz.

The C-V measurement technique has been used to determine impurity profiles inserted into wafers by ion implantation (26)-(29). Both p-n junction and Schottky barrier diodes are used, and results obtained by different authors in different laboratories seem in general to be consistent. The accuracy of the method is quoted to be $\sim \pm$ 10 percent. Typical results are shown in Figure 1. In general, these distributions obtained using C-V techniques are Gaussian near the peaks but have approximately exponential tails. Seidel (27) concluded that these tails are actually present in the impurity distribution since they do not change significantly when measured (by C-V technique) at lower (90 K) temperatures. The range and straggle of the implanted distribution are found to be significantly different from those given by the LSS theory (30), differing up to $\sim$ 35 percent. Kennedy et al. (31) pointed

out that, assuming the validity of the depletion approximation, the differential capacitance technique measures the distribution of the majority carrier concentration rather than the actual distribution of impurity atoms.

Unfortunately, the C-V profiling method is not without its problems. It cannot be used for concentrations above about $10^{18}\ cm^{-3}$, because voltage breakdowns and current leaks occur. Also, it is practically restricted to n-type semiconductors, and cannot measure the concentrations within the initial junction depletion region. The junction depletion region often ends 0.2μm or deeper into the semiconductor. Applying a forward bias voltage would enable concentration measurements closer to the surface, except that at even small forward bias voltages the diffusion of electrons becomes too great. For C-V measurements of p-type material, the barrier height of a Schottky barrier in a p-type material is about 0.5 eV, while the barrier height of a Schottky barrier in an n-type semiconductor is about 0.8 eV. Because of the lower barrier height, one can not apply much reverse bias voltage to a p-type Schottky barrier. Thus one cannot obtain a C-V profile of a p-type material with the reverse bias voltage method.

III. EXPERIMENTS

3.1 Sample preparation

The samples used in this study were prepared and doped before the study began. The substrate materials used were < 100 > oriented undoped or Cr-doped semi-insulating GaAs. The samples were originally cut into 1/4 inch squares from 2 inch curcular wafers of the GaAs. Prior to implantation, each sample was cleaned with basic-H, de-ionized water, trichloroethylene, acetone, and methanol, and dried with blowing nitrogen gas. The substrate was then free-etched with an H_2SO_4 : $30\%H_2O_2$: H_2O solution in a 7:1:1 ratio by volume for 3 minutes. The samples were then ion implanted with Si at room temperature with an incident energy of 100 or 200 keV for a dose of 8×10^{12} or 1×10^{13} $ions/cm^2$. The ion beam was directed at 7 degrees off the < 100 > crystal axis to minimize ion channeling. After implantation, the samples were soaked in an HCl solution for 1 minute to remove a natural oxide layer which had grown since implantation. The samples were then immediately capped with a 1000 $\AA$ layer of Si_3N_4 using a pyrolytic deposition system. Next, the samples were annealed at 800 or 850 °C for 15 minutes in flowing hydrogen gas to activate the implanted ions. This produced the high activation efficiencies, as shown by Kim (18:27), who achieved activation efficencies of at least 80 % for $6 \times 10^{12} cm^{-2}$ Si-implants in GaAs. After annealing, the encapsulants were removed in about 5 minutes by applying a 48 % hydrofluoric acid solution. Each half inch square sample was then cut into 4 quarter inch square samples.

3.2 C–V Measurements and Etching

A series of concentration profiles was measured for each Si implanted GaAs sample using the C–V technique. The samples were etched between the capacitance and voltage measurements to find the carrier concentrations within the initial depletion region of each sample. About ten etches were performed on each sample to

acquire C–V data throughout the initial depletion region. The samples were cleaned before each set of capacitance and voltage measurements, because it was found that the cleaning could very much affect the measurements, especially if a sample was not cleaned for several days.

The C–V data was obtained using the Hewlett–Packard Model 4061 Semiconductor/Component Test System, which was controlled by a 9845B H–P Computer. A sample to be profiled was placed with the implanted face down onto a suction chuck as shown in Figure 9. The suction chuck has three ducts. One duct pulls the air out of a circular groove on the chuck creating a vacuum between the chuck and the sample. Actually, the samples were too small to cover the circular groove, so a sheet of plastic had to be placed over the test chuck and pressed down around the circular groove to obtain a vacuum between the test chuck and the sample. This vacuum pulls the sample down to the chuck and pulls mercury up the other two ducts. The two mercury columns then make metal contacts with the test sample. One mercury duct has a much larger contact area, and was connected to the high side of the bias supply. The smaller mercury duct was connected to the low side. Bias voltages from 0 to -5 or -10 volts were incrementally applied to the sample. The bias voltage was supplied by a Hewlett–Packard 4140B DC Voltage Source. The 4257A multi-Frequency LCR Meter supplied a 0.01 V, 1 MHz test signal to measure the complex impedance and to determine the capacitance of an assumed equivalent circuit. The circuit had the capacitance of the space charge region, or depletion region, in series with the resistance of the material between the two mercury contacts. The capacitance of the larger mercury contact area is much greater than that of the smaller mercury duct contact area, so the measured capacitance is approximately equal to the actual depletion region capacitance. C–V measurements were taken at two positions on each sample, and appeared to change slightly depending on the location of the samples mercury contact area. The C–V measurements were stored on tape in data files, which were then transfered to the AFIT computer system.

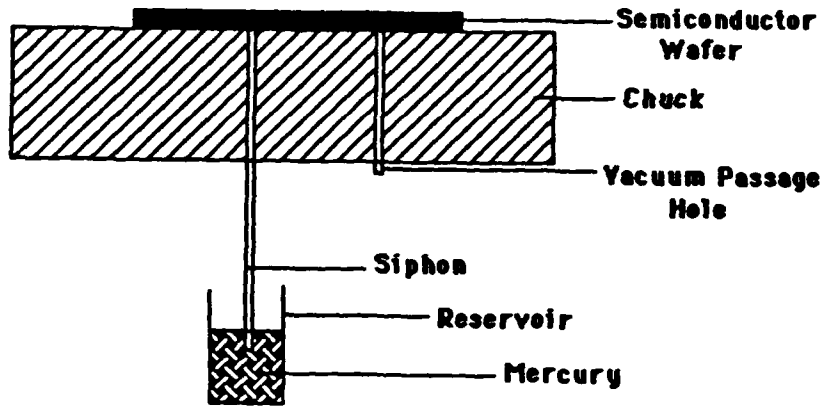

Figure 9. Cross Section of Mercury Contacts

Between the C-V measurements, etching was performed with an H_2SO_4 : $30\%H_2O_2$: H_2O solution in a 1:1:500 ratio by volume at room temperature and with constant stirring. This solution etched about 80 $\mathring{A}$ per minute. Alongside the sample to be etched, two control samples were also etched. The half sections of the control samples were coated with black wax which was not removed until after the last etching. Since the half sections of the control samples under the black wax were not etched, a step height could be measured on these samples as a total etched depth and thus the etch rate could be determined. The etched depth was measured using the Sloan-Dektak IIA Surface Profiling System.

3.3 PN 4200 Polaron's Semiconductor Profiler

To produce an electronic device from a semiconductor, it is generally necessary to engineer impurity concentration changes in the surface layers of the material. These changes take many forms depending on the semiconductor material used, and the device that it is intended to produce, but usually either the bulk material's

surface is altered by some form of chemical diffusion or particle bombardment, or new layers of semiconductor material are deposited or grown onto the surface of the bulk.

Whatever the process used to engineer these impurity concentration changes, the results are dependent on the purity of the starting materials and the physical conditions of the process (energy of implantation, temperature of diffusion, etc.). Also, although the process may have achieved the correct chemical impurity concentration changes with depth into the surface, the successful operation of the semiconductor device depends on the eletrical activity of the species introduced. The Polaron PN 4200 is a computer controlled electrochemical carrier concentration profiling system for obtaining electrically active carrier concentration profiles against depth into the semiconductor surface and provides a convenient (and often the only) way to check the efficiency and success of the initial processing before the expensive and time consuming device manufacturing stage begins.

The Polaron PN 4200 utilizes the capacitance-voltage data obtained from an electrochemical Schottky barrier, while electrochemical dissolution is induced to obtain majority carrier concentration against depth profiles of semiconductor materials. This technique, first developed by Faktor and Ambridge at British Telecom Research Laboratories, enables electrically active profiles to be obtained through large depths of material with high resolution and over many orders of magnitude of carrier concentrations.

The system operates by placing the sample in contact with a defined area of electrolyte and applying a small biasing voltage across the semiconductor/electrolyte interface. As this contact is basically equivalent to a metal Schottky contact, information about the majority carrier concentration can be obtained by analyzing capacitance voltage data from the depletion region.

By formulating the electrolyte in such a way that a well defined electrochemical dissolution reaction can be induced, the area of semiconductor material in contact

with the electrolyte can be gradually dissolved. A carrier concentration against depth profile can be constructed without necessitating the bias voltage increases inherent with conventional depletion profiling systems.

A series of concentration profiles was measured for each Si implanted GaAs sample using the C-V technique. The samples were etched between the capacitance and voltage measurements to find the carrier concentrations within the initial depletion region of each sample without moving. While the polaron profiler etched chemically only one point on the sample for each etching, the mercury dot C–V profiler etched chemically whole sample for each etching.

The experimental procedure is as follows. Clean the electrochemical cell body well in deionized water to remove all traces of the previous electrolyte and re-assemble the contacts. Carefully mount the cell onto the cellmounting tray, inserting a piece of filter paper between the sealing ring and the back contact pins to absorb any liquid ejected from the pump. Remove the filter paper and blow dry the sealing ring and back contacts. Clean and dry the sample and select the area for the etch. Carefully place the sample with its measuring surface facing the sealing ring, and lightly pull and twist the back contact plunger until the key allows it to slide back in. After mounting the sample on the electrochemical cell, inject 7 or 8 *mls* NaOH:EDTA solution at room temperature in a 2:1 ratio by volume on the hole. Put the saturated calomel electrode on the hole of the electrochemical cell. After that, run the HP 86B computer with polaron profiler software package.

The PN 4200 Polaron Profiler can obtain the carrier concentration either by depletion profiling or etch profiling. In the depletion profiling, carrier concentration and depletion depth are measured as a function of voltage. The maximum depth probed will depend on the carrier concentration, the material, and the maximum reverse voltage applied. There are 20 voltage steps, and the measurement proceeds from the cathodic to the anodic voltage limits. Current limits are also in effect to terminate the measurement if necessary. The d.c. bias necessary to measure the

carrier concentration, and also necessary to induce controlled electrochemical etching has been determined from the C/V and I/V curves, and it is possible to obtain an etch profile.

In order to find the carrier concentrations within the initial depletion region of sample, it is necessary to get a series of whole profiles for each etching. The PN 4200 Polaron Profiler can obtain both the depletion profile and etch profile by calculating the C-V data automatically. However, it is not programed to get a series of whole profiles for each etching. For obtaining a series of whole profile for each etching, the procedure are as follows. 1) Carry out the depletion profiling. 2) Execute the etch profiling. 3) After etching the sample, halt the system. 4) Carry out the depletion profiling. 5) Continue this process until the required etched depth is reached. However, the PN 4200 Polaron Profiler cannot obtain the whole profile C-V data for each etching. Therefore, the PN 4200 Polaron Profiler cannot be used for this research.

IV. THEORY

There are three possible methods to be developed for determining the charge carrier concentration within the initial depletion region. They are the Charge Density Moment Method, the Voltage Second Derivative Method, and the Voltage First Derivative Method (32). In this research, the Charge Density Moment Method has been studied in detail. The Charge Density Moment Method is very sensitive to experimental error.

4.1 Charge Density Moment Method

When a metal is brought into contact with an n-type semiconductor under a reverse bias voltage V, the potential Ψ varies with depth into the semiconductor as shown in Figure 10. The potential falls off steeply and then levels off at a distance x_w. E_C is the conduction band minimum at x_w, and E_{FS} is the Fermi energy level at x_w. Q or e is the electronic charge, and V_{bi} is the built-in potential. The depletion region extends from x=0 to $x=x_w$. As seen by equation (4), the built-in potential depends on the endpoints x=0 and $x=x_w$. The potential V is governed by Poisson's equation:

$$-\frac{d^2V}{dx^2} = \frac{\rho(x)}{\epsilon} = \frac{eN(x)}{\epsilon} = \frac{dE}{dx}, \tag{8}$$

where ρ(x) is the charge density at x, ϵ is the permittivity of the semiconductor, N(x) is the carrier concentration given by equation (3) at x, and E is the electric field.

By integrating Poisson's equation once, the electric field is found to be

$$E(x) = -\frac{dV(x)}{dx} = -\frac{e}{\epsilon}\int_x^{x_w} N(x)dx + E_W, \tag{9}$$

where E_W is the electric field at x_w (19:209). By integrating a second time, the voltage drop from the surface to x_w is shown to be

$$V + V_{bi} = \frac{e}{\epsilon}\int_0^{x_w}\int_x^{x_w} N(x)dx^2 - x_w E_W, \tag{10}$$

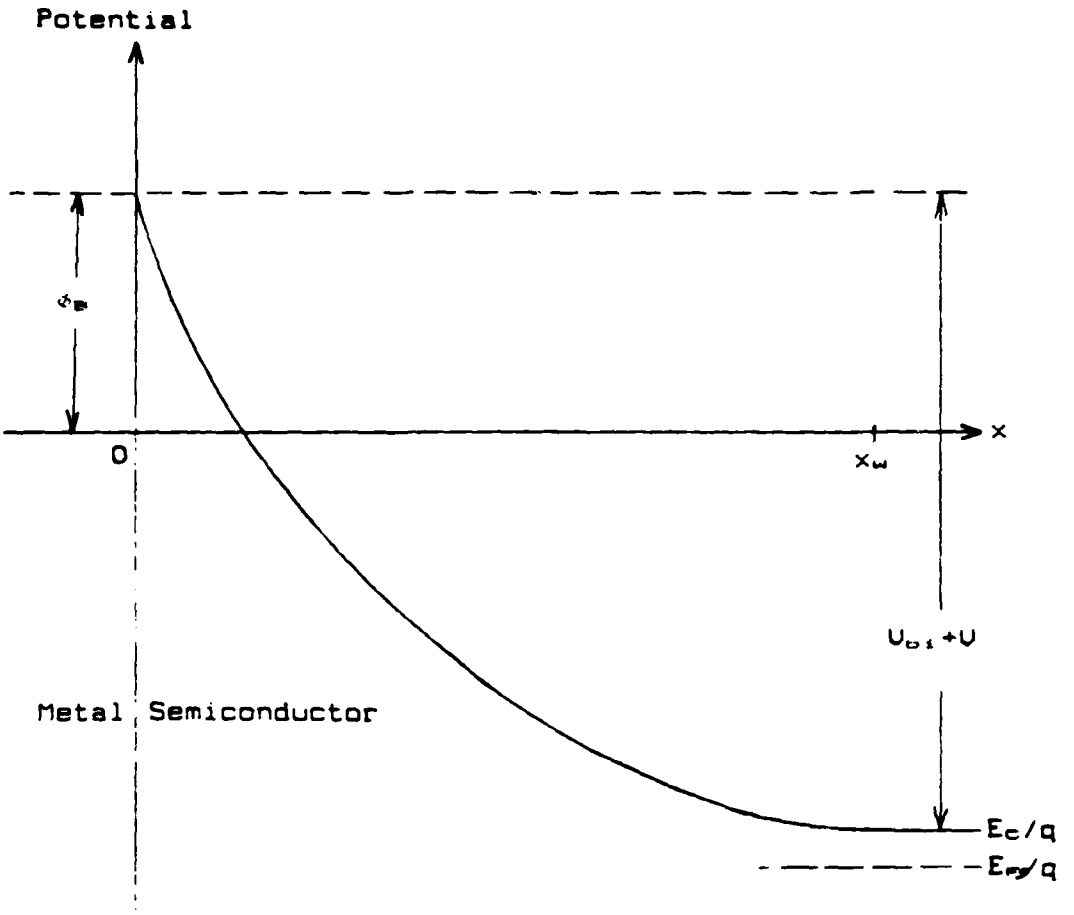

Figure 10. Potential Diagram of Metal-Semiconductor Contact

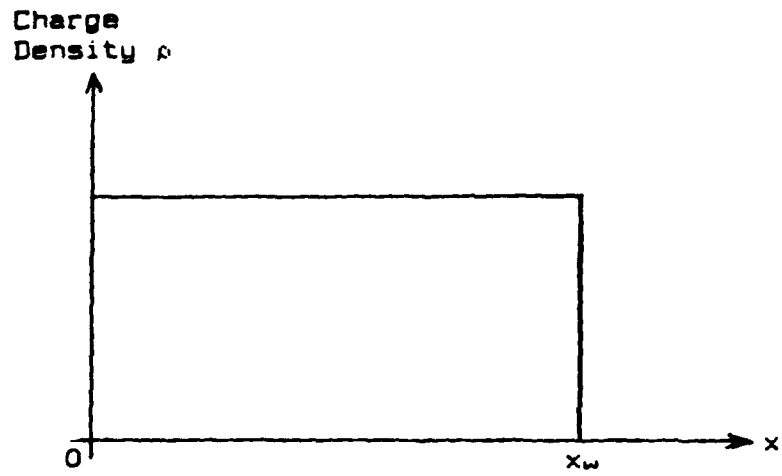

Figure 11. Abrupt Approximation of Depletion Region

where V is the applied reverse bias voltage required to extend the depletion region to x_w, and the reverse bias voltages are considered positive. Giacoletto (19:210) pointed out that this double integral can be integrated by parts to yield

$$V + V_{bi} = \frac{e}{\epsilon} \int_0^{x_w} xN(x)dx - x_w E_W, \tag{11}$$

which relates the applied voltage to a moment of the charge density. If the depletion region is assumed to end abruptly as shown in Figure 11, then E_W is zero, since there are no charges right of x_w. Actually, the depletion region ends gradually, as shown in Figure 12, due to an electron *tail* at x_w (20:74-77). The electron concentrations near x_w are usually considered small and the abrupt approximation applied, so that E_W is considered negligible (22:790). With the E_W term deleted, equation (11) becomes

$$V + V_{bi} = \frac{e}{\epsilon} \int_0^{x_w} xN(x)dx. \tag{12}$$

Equations (9), (10), and (11) were based on the Giacoletto's (19) method for solving the Poisson's equation. Equation (12) was based on the usual method

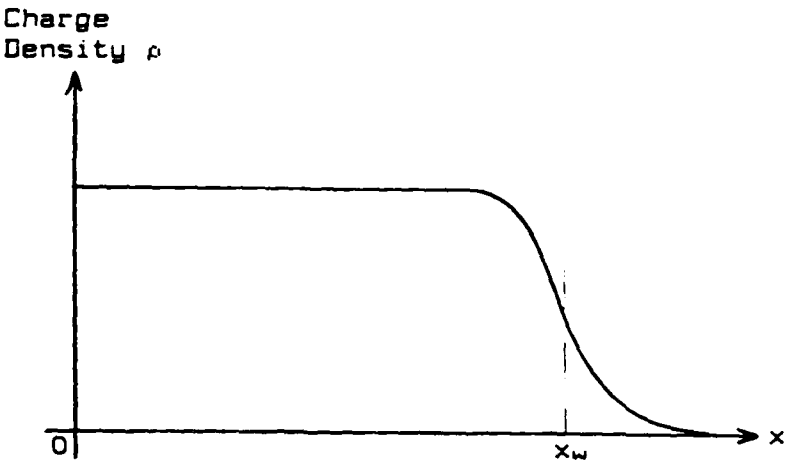

Figure 12. Gradual Ending of Depletion Region

applying the abrupt depletion approximation. There are some differences between the Giacoletto's method and usual solutions of Poisson's equation, as shown in Table 1. From equation (12), it can be seen that even if one measures V, V_{bi}, and x_w, an infinite number of N(x) profiles could give the same result.

Giacoletto (19:215) also showed that the voltage drop from a position x_o to x_w is

$$V(x_o) - V(x_w) = \frac{e}{\epsilon}\int_{x_o}^{x_w}(x - x_o)N(x)dx + (x_w - x_o)E_W, \tag{13}$$

where x_o is between 0 and x_w. If x_w is far from both x=0 and x=x_o and if the material is etched between the surface and x_o, then E_W and the shape of the space charge region as shown in Figure 12 should change very little. Under these circumstances, it can be seen from equation (13), that the potential drop from x_o to x_w is the same regardless of whether the material has been etched away between 0 and x_o. Where equation (13) is applied to the abrupt depletion approximation,

$$V(x_o, x_w) + V_{bi}(x_o, x_w) = \frac{e}{\epsilon}\int_{x_o}^{x_w}(x - x_o)N(x)dx, \tag{14}$$

Table 1. Comparison between Giacoletto's and Usual Solutions of Poisson's Equation

Giacoletto's	*Usual Solution*
$N(x) = N_d(x) - N_a(x)$	$N(x) = N_d(x) - N_a(x)$
$\frac{d^2V(x)}{dx^2} = -\frac{e}{\epsilon}N(x)$	$\frac{d^2V(x)}{dx^2} = -\frac{e}{\epsilon}N(x)$
Boundary Condition $E(x)\|_{x=W} = E_W$, where $E_W = -\frac{KT}{e}\frac{\frac{dN(x)}{dx}}{\sqrt{N^2(x)+4n_i^2}}\|_{x=W}$	$E(x)\|_{x=W} = -\frac{dV(x)}{dx}\|_{x=W} = 0$
$\frac{dV(x)}{dx} = \frac{e}{\epsilon}\int_{x=x}^{x=W} N(x)dx - E_W$	$\frac{dV(x)}{dx} = \frac{e}{\epsilon}\int_{x=x}^{x=W} N(x)dx$
Boundary Condition $V(x)\|_{x=W} = V_W$	$V(x)\|_{x=W}=V_{bi}$ $(= V_{bi}+ V_{RB})$ $V(x)\|_{x=W}=V_{bi}=\frac{e}{\epsilon}\int_0^W xN(x)dx$
Boundary Condition $V(x)\|_{x=0}$ $= V_W + W E_W - \frac{e}{\epsilon}\int_0^W xN(x)dx$ $= V_{RB} + \phi_b$	$V(x)\|_{x=0} = 0$
Boundary Condition	$[\varepsilon_C - \varepsilon_F]_{x=W}$ $= \frac{1}{2}\Delta\varepsilon - \frac{KT}{e}ln[\frac{m_h^*}{m_e^*}]^{\frac{3}{4}} - \frac{KT}{e}\sinh^{-1}[\frac{N(x)}{2n_i}]_{x=W}$ $= -KTln[\frac{N(x)}{N_C}]_{x=W}$ $= -eV(x)\|_{x=W} + e\phi_b = e\phi_b - eV_{bi}$
Within the Depletion Region	$V(x) = -\frac{1}{e}[\varepsilon_C(x) - \varepsilon_F - e\phi_b]$ $= \frac{1}{e}[e\phi_b - \{\varepsilon_C(x) - \varepsilon_F\}]$
Solution of Poisson's Equation $V(x) = \frac{e}{\epsilon}\{\int xN(x)dx - \int_0^W xN(x)dx\}$ $+\frac{e}{\epsilon}x\int_x^W N(x)dx + E_W(W-x) + V_W$	$V(x) = \frac{e}{\epsilon}\int xN(x)dx + \frac{e}{\epsilon}x\int_x^W N(x)dx$
With Reverse Bias Voltage	$V(x)\|_{x=W} = V_{bi} + V_{RB}$ $= \frac{e}{\epsilon}\int_0^W xN(x)dx$

where $V(x_o, x_w)$ and $V_{bi}(x_o, x_w)$ are the applied voltage and built-in potential, respectively.

If one designates the ith etch thickness as t_i and the distance of the ith etched surface from the original unetched surface as T_i, then

$$T_i = \sum_{j=0}^{i} t_j, \qquad and \qquad T_o = 0. \tag{15}$$

The potential difference between T_i and x_w is

$$V(T_i, x_w) + V_{bi}(T_i, x_w) = \frac{e}{\epsilon} \int_{T_i}^{x_w} (x - T_i) N(x) dx, \tag{16}$$

where x_w is a common reference depth. The built-in potential in thermal equilibrium V_i^{bi} after the ith etching can be obtained with zero applied voltage using the boundary condition :

$$\epsilon V_i^{bi} = e\phi_B - KTln[\frac{N_C}{N(x)}] \qquad at \qquad x = T_i + W_{i,0}, \tag{17}$$

where ϕ_B is a barrier potential and $W_{i,0}$ is an initial depletion width after the ith etch. Therefore, equation (16) is changed to

$$V_{i,j}^{RB} + V_i^{bi} = \frac{e}{\epsilon} \int_{x=T_i}^{T_i + W_{i,j} = x_w} (x - T_i) N(x) dx. \tag{18}$$

There are various ways equation (18) can be used to find the concentration N(x) within the initial depletion region. For the (i-1)th etching, the voltage drop from the total etched depth T_{i-1} to x_w is

$$V_{i-1,m}^{RB} + V_{i-1}^{bi} = \frac{e}{\epsilon} \int_{T_{i-1}}^{x_w} (x - T_{i-1}) N(x) dx. \tag{19}$$

As shown by equation (17), the built-in potential V_{bi} depends on the barrier potential ϕ_B and the carrier concentration N(x) at $x = T_i + W_{i,0}$. If one assumes that the barrier potential ϕ_B is the same for each etch depth, and if one uses x_w as a common reference, then the built-in potentials are not the same :

$$V_i^{bi} \neq V_{i-1}^{bi}. \tag{20}$$

Subtracting equation (18) from equation (19) yields

$$V_{i-1,m}^{RB} - V_{i,j}^{RB} + (V_{i-1}^{bi} - V_i^{bi})$$

$$= \frac{e}{\epsilon}\int_{T_{i-1}}^{x_w}(x - T_{i-1})N(x)dx - \frac{e}{\epsilon}\int_{T_i}^{x_w}(x - T_i)N(x)dx, \tag{21}$$

which can be expressed as

$$\int_{T_{i-1}}^{T_i}(x - T_{i-1})N(x)dx$$

$$= \frac{e}{\epsilon}[(V_{i-1,m}^{RB} - V_{i,j}^{RB}) + (V_{i-1}^{bi} - V_i^{bi})] - (T_i - T_{i-1})\int_{T_i}^{x_w} N(x)dx. \tag{22}$$

If the Nth etch depth T_N is the distance very close to but beyond the end of initial depletion region of the original unetched surface, as shown in Figure 13, then

$$\int_{T_{N-1}}^{T_N}(x - T_{N-1})N(x)dx$$

$$= \frac{e}{\epsilon}[(V_{N-1,m}^{RB} - V_{N,j}^{RB}) + (V_{N-1}^{bi} - V_N^{bi})] - t_N\int_{T_N}^{x_w} N(x)dx, \tag{23}$$

where t_N is the nth etch thickness between the etch depths. The quantities on the right side of equation (23) are all measureable or known. If the etch thicknesses t_N are small, the concentration N(x) can be treated as uniform or constant between the etch depths, and the integral on the left side of equation (23) can then be evaluated :

$$\int_{T_{N-1}}^{T_N}(x - T_{N-1})N(x)dx = \frac{N_N}{2}t_N^2. \tag{24}$$

So, the equation solved for N_N to give

$$N_N = \frac{2}{t_N^2}\{\frac{\epsilon}{e}[(V_{N-1,m}^{RB} - V_{N,j}^{RB}) + (V_{N-1}^{bi} - V_N^{bi})] - t_N\int_{T_N}^{x_w} N(x)dx\}, \tag{25}$$

and this value of N_N can be assigned to the midpoint of the two etch depths :

$$x = \frac{T_{N-1} + T_N}{2}. \tag{26}$$

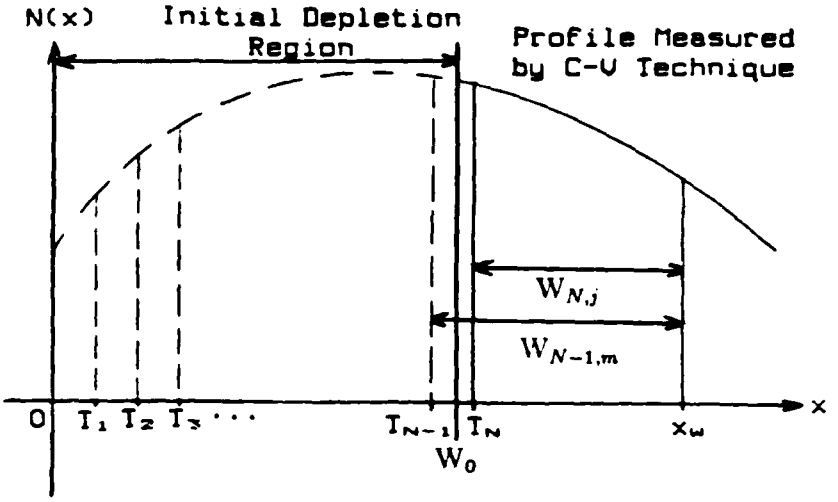

Figure 13. Etch Depths Across Carrier Profile

With N(x) known between T_{N-1} and T_N, the same method can then be applied to find N(x) between T_{N-2} and T_{N-1}. This method can be repeatedly applied working backward to the original unetched surface.

Since this method treats the concentration as uniform between each etch depth, the value of the concentration will be slightly different from the exact value. If the value calculated for the concentration within one etch layer is smaller than the exact value, the calculated value in the next etch layer will be compensated by being higher than its exact value. Thus, the concentrations calculated by the Charge Density Moment Method may oscillate about the exact profile. In this case, a best fit curve should be obtained. Another disadvantage of this method is that it cannot be applied until after the end of the initial depletion region has been etched.

V. COMPUTER PROGRAMS

The computer programs shown in Appendices B and C implement the methods developed in the previous chapter and use capacitance–voltage data to calculate the carrier concentrations within the initial depletion region of semiconductors. To better analyze these methods, files of ideal capacitance–voltage data were computer generated. Appendix A shows a computer program used to generate ideal capacitance–voltage data files for an LSS Gaussian dopant distribution. For the Linear and Parabolic function dopant distribution case, only the function part of ideal capacitance–voltage data generation program was changed as shown in Appendix A. Appendix D shows a computer program used to calculate the initial depletion widths for an LSS Gaussian dopant distribution. This program found the initial depletion widths by self-consistently averaging the doping profile within the depletion region and solving Poisson's equation.

In the ideal capacitance–voltage data generation program, the carrier concentration equation (6) could be applied in reverse to create the ideal C–V data. However, it was found that the carrier concentration was deduced from the average capacitance $\overline{C}$ rather than just C. Thus the equation (6) can be rewritten as

$$\frac{dC}{dV} = \frac{-\overline{C}^3}{\epsilon\epsilon_0 q A^2 N(x)} \tag{27}$$

by using

$$\overline{C} = \epsilon\epsilon_0 A/x, \tag{28}$$

where 13.1 is used as a value of ϵ, 2.04 $\times 10^{-3} cm^2$ is used as a value of A. In these equations (27) and (28), $\overline{C}$ was an average value. Initial depletion width was entered using the initial depletion width calculation program as shown in Appendix D. This program also calculated the built-in potential (V_{bi}) by using

$$V_{bi}(i) = \phi_B - \frac{KT}{e} ln[\frac{N_C}{N(x)}] \quad at \quad x = W(i,1) + T(i), \tag{29}$$

where 0.8 volt was used as a barrier potential value of ϕ_B, W(i,1) is an initial depletion width after the ith etch, and T(i) is a total etched depth after the ith etch. Since equations (27), (28), and (29) are the same types of equations as were used in developing the methods of finding the initial depletion width concentrations, the methods could be proven using the ideal computer generated capacitance–voltage data. The methods were based on the same assumptions as the regular C-V technique, and the ideal data could still be used in analyzing the methods and the effects of experimental error. The capacitance after the ith etch were easily calculated as

$$C(i,j) = 2\overline{C}(i,j) - C(i,j-1), \tag{30}$$

where C(i,j) is the ith capacitance after the ith etch. The jth distance from the original unetched surface was calculated as

$$x(i,j) = W(i,1) + (j-1)H + T(i), \tag{31}$$

where H is a small distance interval of capacitance–voltage data. The difference of reverse bias voltages (dV) were calculated from equation (27). The jth reverse bias voltage after the ith etch were determined from

$$V^{RB}(i,j) = V^{RB}(i,j-1) + dV, \tag{32}$$

where the zeroth reverse bias voltage was set at 0: $V^{RB}(i,0) = 0$. The reverse bias voltage increments were added to this starting reverse bias voltage to obtain the applied bias voltages. In order to obtain the correct initial depletion profile, it was necessary to change from reverse bias voltages to average reverse bias voltages. The average reverse bias voltage and carrier concentration pairs using the capacitance–voltage data were stored in a data file for the ith etch. Usually, 11 data files were created for 10 etches with either 100 $\AA$ or 200 $\AA$ etching step.

To calculate the carrier concentrations from the experimental data files by the normal C–V technique, the finite difference form of equation (6) was used :

$$N(x) = \frac{[V^{RB}(i,j-1) - V^{RB}(i,j)]}{\epsilon\epsilon_o q A^2 [C(i,j) - C(i,j-1)]} [\overline{C}(i,j)]^3, \tag{33}$$

where

$$x = T(i) + \frac{\epsilon\epsilon_o A}{\overline{C}(i,j)} \quad . \tag{34}$$

As expected, the profiles calculated by the C–V technique after each etching overlapped exactly for the ideal C–V data.

The computer programs used to find the depletion region concentrations all required a measure of $\overline{V}^{RB}$(i,XE), the average reverse bias voltage necessary to extend the depletion region from the 1st depth after the ith etch, x(i,1) to the common reference distance XE. $\overline{V}^{RB}$(i,XE) could then be found through linear or spline interpolation between these distances. The carrier concentration at the common reference distance XE could be also found by using same method. This program found the potential differences between etch layers with common depletion right edge of XE. The integral in equation (25) could be calculated by using numerical analysis:

$$\int_{T_i}^{XE} N(x)dx = \sum_{x=T_i}^{XE} N(x)\,\Delta\,x. \tag{35}$$

For plotting, this program used Metalib, which is a high level graphics support library for Fortran. It provides facilities for simple two-dimensional data plots, as well as more complex features such as isolevel tracing, curve fitting, and plotter symbols. It is possible to display the output by using an Imagen laser printer and a Versatec printer/plotter.

VI. RESULTS AND DISCUSSION

This chapter explains the results for the ideal C-V data, experimental C-V data and the Polaron Profiler. The results for the ideal C-V data covered a Linear, Parabolic and LSS Gaussian function to find the carrier concentrations within the initial depletion region of the metal-semiconductor contact using the Charge Density Moment Method. The results for experimental C-V data covered the Si implants in GaAs implanted at 100 keV to a dose of $8\times10^{12}/cm^2$ to find carrier concentrations within the initial depletion region of the semiconductor using the Charge Density Moment Method. For the ideal C-V data and experimental C-V data, this research was very succesful except for some experimental errors. The results for the Polaron Profiler deal with Si implants in GaAs implanted at 100 keV to a dose of $1\times10^{13}/cm^2$. As mentioned previously, the Polaron Profiler could not be used to find the carrier concentrations within the initial depletion region.

6.1 Results for Ideal C-V Data

Figures 14 to 17 show the performance of the Charge Density Moment Method for a linear profile. The calculated carrier concentrations in the depletion region for an etch depth of 100 $\AA$ per layer oscillated more than expected about the true curve, as shown in Figures 14 and 15. However, the calculated carrier concentrations in the depletion region for an etch depth of 200 $\AA$ per layer were very similar to the true curve as shown in Figures 16 and 17. In Figures 14 to 17, the common reference point was changed for an etch depth of 100 $\AA$ and 200 $\AA$ as shown in Figures 15 and 17.

Figures 18 to 21 show the performance of the Charge Density Moment Method for a parabolic profile. The calculated carrier concentrations within the initial depletion region for an etch depth of 100 $\AA$ per layer oscillated more than expected about the true curve, as shown in Figures 18 and 19. On the contrary, the calculated

carrier concentrations within the initial depletion region for an etch depth of 200 $\AA$ per layer were very much similar to the true curve as shown in Figures 20 and 21. Figures 18 and 20 show that the reference point is as near as possible to the minimum distance of theoretical reference point. Figures 19 and 21 also show that the reference point is near to the maximum x.

Figure 22 shows the performance of the Charge Density Moment Method for the LSS profile for Si implants in GaAs implanted at 100 keV to a dose of $1\times10^{13}/cm^2$. In this figure, the etch depth is 118 $\AA$ per layer and the reference point is 0.235 μm. Etch depth was calculated from the Initial Depletion Width Calculation program shown in Appendix D. For this figure, the calculated carrier concentrations within the depletion region were very similar to the true curve. Figures 23 and 24 show the performance of the Charge Density Moment Method for the LSS profile of Si implants in GaAs implanted at 100 keV to a dose of $6\times10^{12}/cm^2$. The calculated carrier concentrations in the depletion region overlapped those of the true curve. The reference point is near to the minimum point of the theoretical reference point X_o shown in Figure 23, and the maximum x shown in Figure 25. Figures 25 to 27 show the performance of the Charge Density Moment Method for the LSS profile for Si implants in GaAs implanted at 200 keV to a dose of $4\times10^{12}/cm^2$. In Figure 25, etched depth is 100 $\AA$ per each layer. The calculated carrier concentrations in the depletion region oscillated as shown in Figure 25. In Figures 26 and 27, etch depth is 200 $\AA$ per layer, and the calculated carrier concentrations in the depletion region were much more similar to the true curve. Eleven C-V data files were needed to calculate the carrier concentrations in the depletion region as shown in Figure 25, but only six C-V data files for Figures 26 and 27.

In Figures 14 to 27, the calculated carrier concentrations in the depletion region for an etch depth of 100 $\AA$ oscillated more than expected about the true profile. Once again, the calculated carrier concentrations within the initial depletion region for an etch depth of 200 $\AA$ were the same as the true profile. The amount of oscillation

varied with the choice of the etch depth t. This was because of inaccuracies in the differences of the reverse bias voltages between etched layers with the common reference point caused by the use of too small of a step size in generating the ideal C-V data. From these results, 200 $\AA$ is the best etch depth for ideal C-V data. It was very economical and efficient to calculate the carrier concentration within the initial depletion region as shown in Figures 25 and 26. However, there are some disadvantages to using an etch depth of 200 $\AA$ per layer for ideal C-V data. First, one could not calculate the carrier concentrations in depths between 0 and 200 $\AA$. Second, the calculated carrier concentrations are a little higher than those of the true profile within the depletion region. Also, there were no differences in the changed common reference point. This was because the C-V data was ideal data which was generated by using the computer program. As expected, the profiles calculated by the C-V technique, for the different etches, overlapped exactly for the ideal C-V data as shown in Figures 14 to 27.

The Charge Density Moment Method cannot be applied until after etching to the end of the initial depletion region. This method required an integration to find the area under the profile from the edge of the depletion region to the common reference point. Also, this method required differences of reverse bias voltage between etch layers with a common reference point to calculate the carrier concentration within the depletion region. Figures 14, 15 and 25 show the results of the Charge Density Moment Method when the voltages of each etching layer were purposely offset by 1 mV, and demonstrate that the Charge Density Moment Method is very sensitive. However, for the ideal C-V data, this method was very successful in calculating the carrier concentrations within the initial depletion region. Thus, this method was attempted on experimental C-V data.

6.2 Results for Experimental C-V Data

Figures 28 to 30 show the performance of the Charge Density Moment Method for Si implants in GaAs implanted at 100 keV to a dose of $8\times10^{12}/cm^2$. In these figures, the etch depth was 136 $\AA$ per layer. During the experiment, the best etch depth was determined to be between 100 $\AA$ and 300 $\AA$. As etch depth increased beyond 136 $\AA$, carrier concentrations for each etching got worse, because the carrier concentrations for each etching did not overlap each other. The profiles for the different etches overlapped only approximately as shown in Figures 28 to 30. For this reason, the calculated carrier concentrations within the initial depletion region given by the Charge Density Moment Method oscillated much more than the experimental data as shown in Figures 28 and 30. This was also because of inaccuracies in the differences of reverse bias voltages and built-in potential between etch layers caused by inaccurate experimental C-V data. However, the calculated carrier concentrations within the initial depletion region were very similar to the expected curve as shown in Figure 29. This was because the profiles obtained for the different etches at the reference point 0.3 μm overlapped exactly for the experimental data as shown in Figure 29. As mentioned previously, there were no differences as the reference point was changed for the ideal C-V data. However, for the experimental C-V data, the location of the reference point was very important, because the profiles obtained for the different etches at the reference point must overlap exactly to obtain the best results.

These experimental C-V data includes a few corrected C-V data from experimental errors. The few C-V data with experimental errors were corrected to calculate the carrier concentrations within the depletion region. This was because the Charge Density Moment Method was very sensitive to experimental errors. These errors are a sample cleanliness, operator errors, and mechnical errors. Therefore, for the best results, operator should get rid of experimental errors in generating the experimental C-V data.

6.3 Results for Polaron Profiler

Figure 31 shows the depletion profile for Si implants in GaAs implanted at 100 keV to a dose of $1\times10^{12}/cm^2$ using the Polaron Profiler. The Polaron Profiler which was developed in recent years could not calculate the carrier concentrations within the initial depletion region of a metal-semiconductor contact. The profiles for the different etches overlapped only approximately as shown in Figure 31. In the depletion profiling, it could not display the etched depth, profiles, and C-V data on the screen. For comparison with depletion profiling and etch profiling, these were different in doping concentrations and in the initial depletion widths after each etching. Also, it is difficult to get whole profile for each etching. The Polaron Profiler could not generate the C-V data for profiling. This was because the operating program could not operate automatically this process. For these reasons, it was not used to find the carrier concentrations within the depletion region.

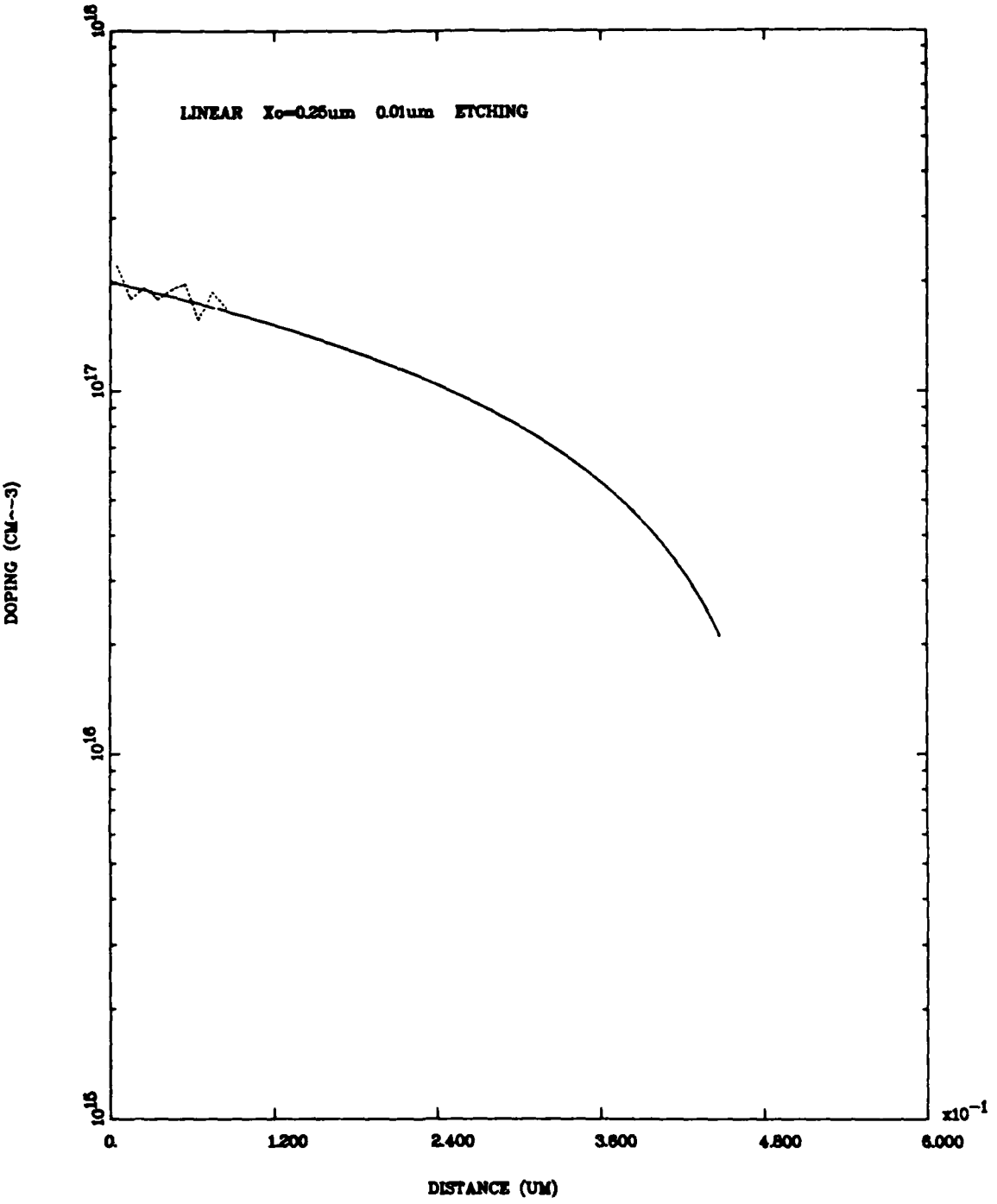

Figure 14. Performance of the Charge Density Moment Method for a Linear Profile (Etched Depth Step: 100$\mathring{A}$, Reference Point: 0.25μm)

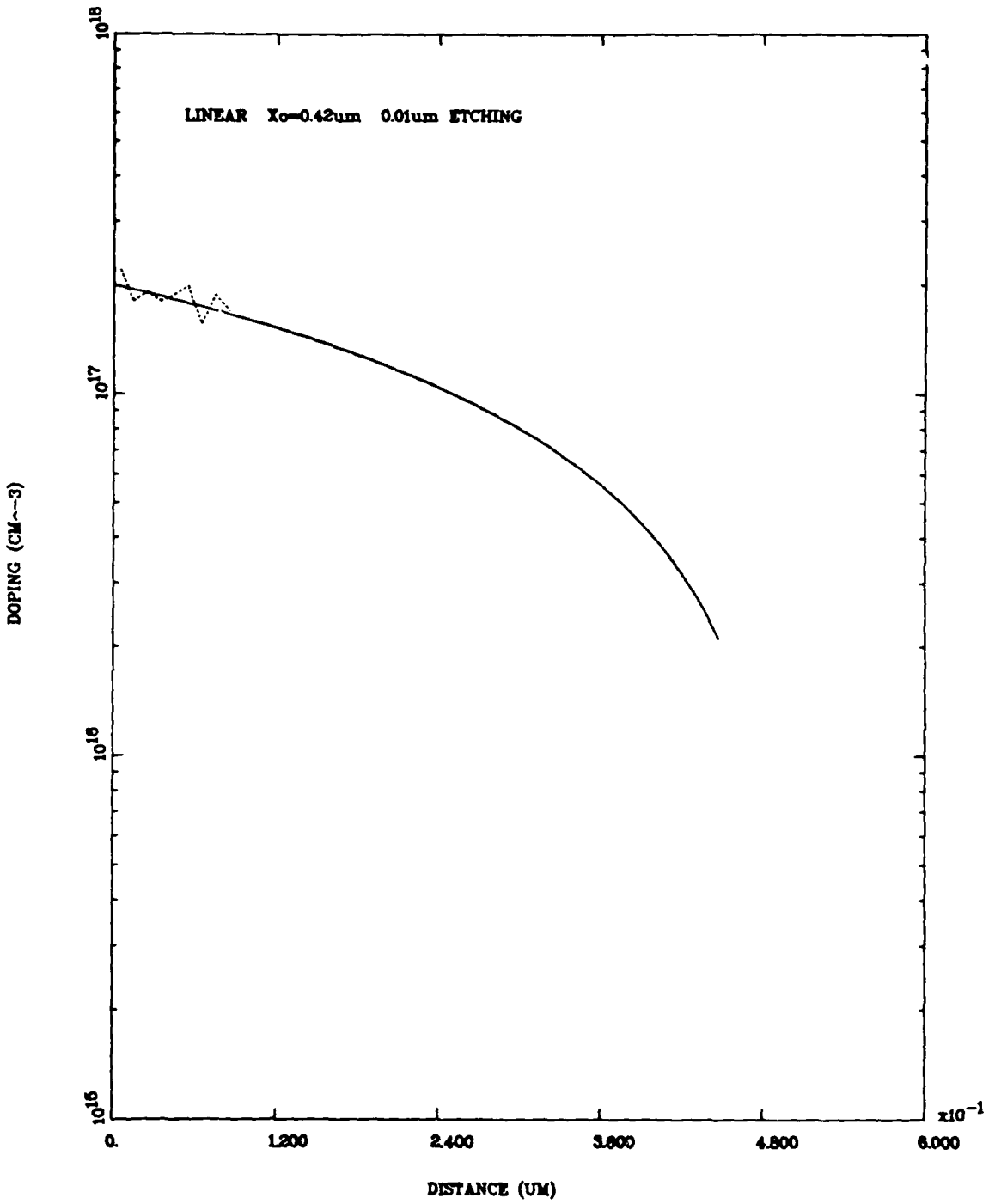

Figure 15. Performance of the Charge Density Moment Method for a Linear Profile (Etched Depth Step: 100$\AA$, Reference Point: 0.42μm)

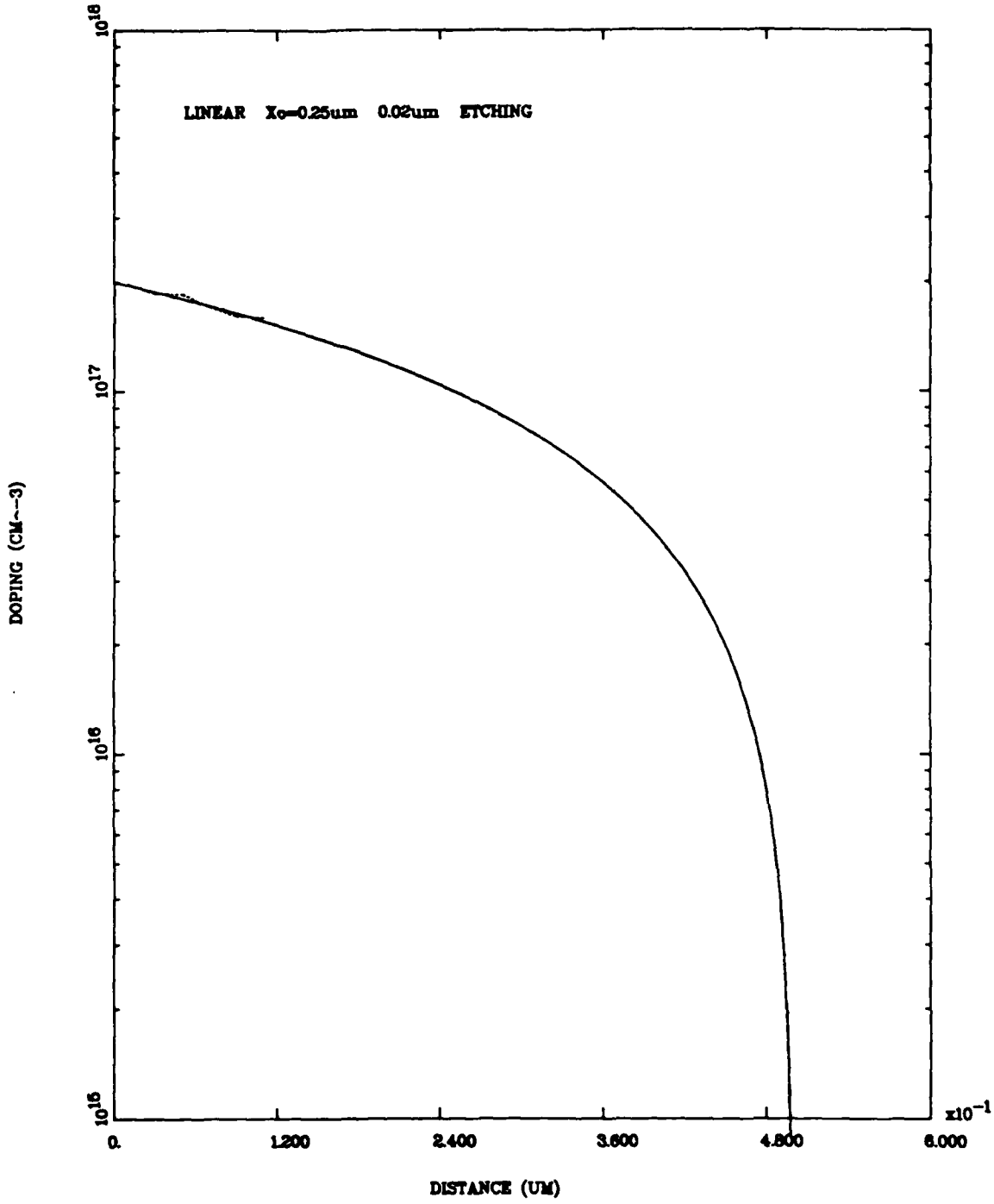

Figure 16. Performance of the Charge Density Moment Method for a Linear Profile (Etched Depth Step: 200$\mathring{A}$, Reference Point: 0.25μm)

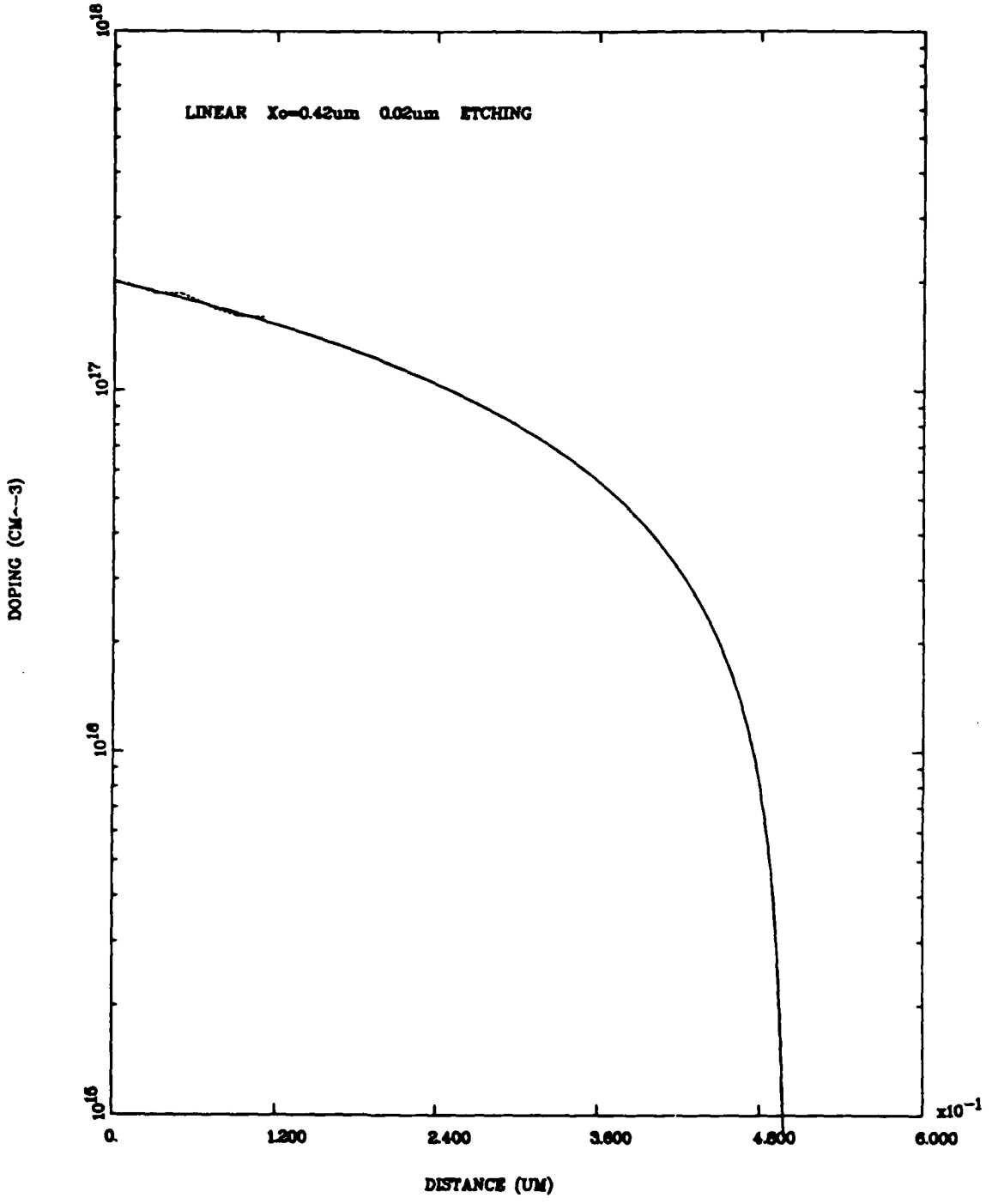

Figure 17. Performance of the Charge Density Moment Method for a Linear Profile (Etched Depth Step: 200$\mathring{A}$, Reference Point: 0.42μm)

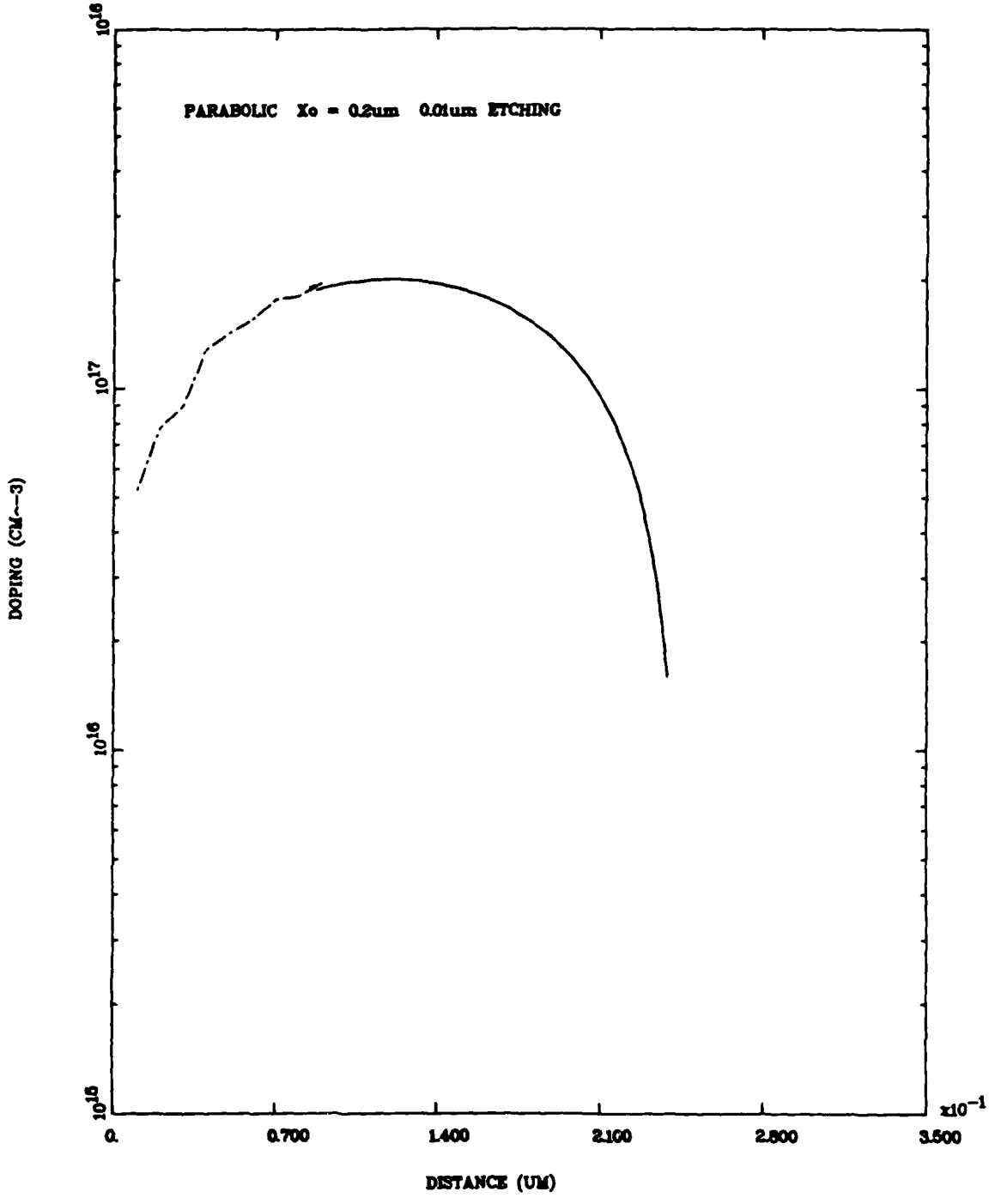

Figure 18. Performance of the Charge Density Moment Method for a Parabolic Profile (Etched Depth Step: 100$\mathring{A}$, Reference Point: 0.2μm)

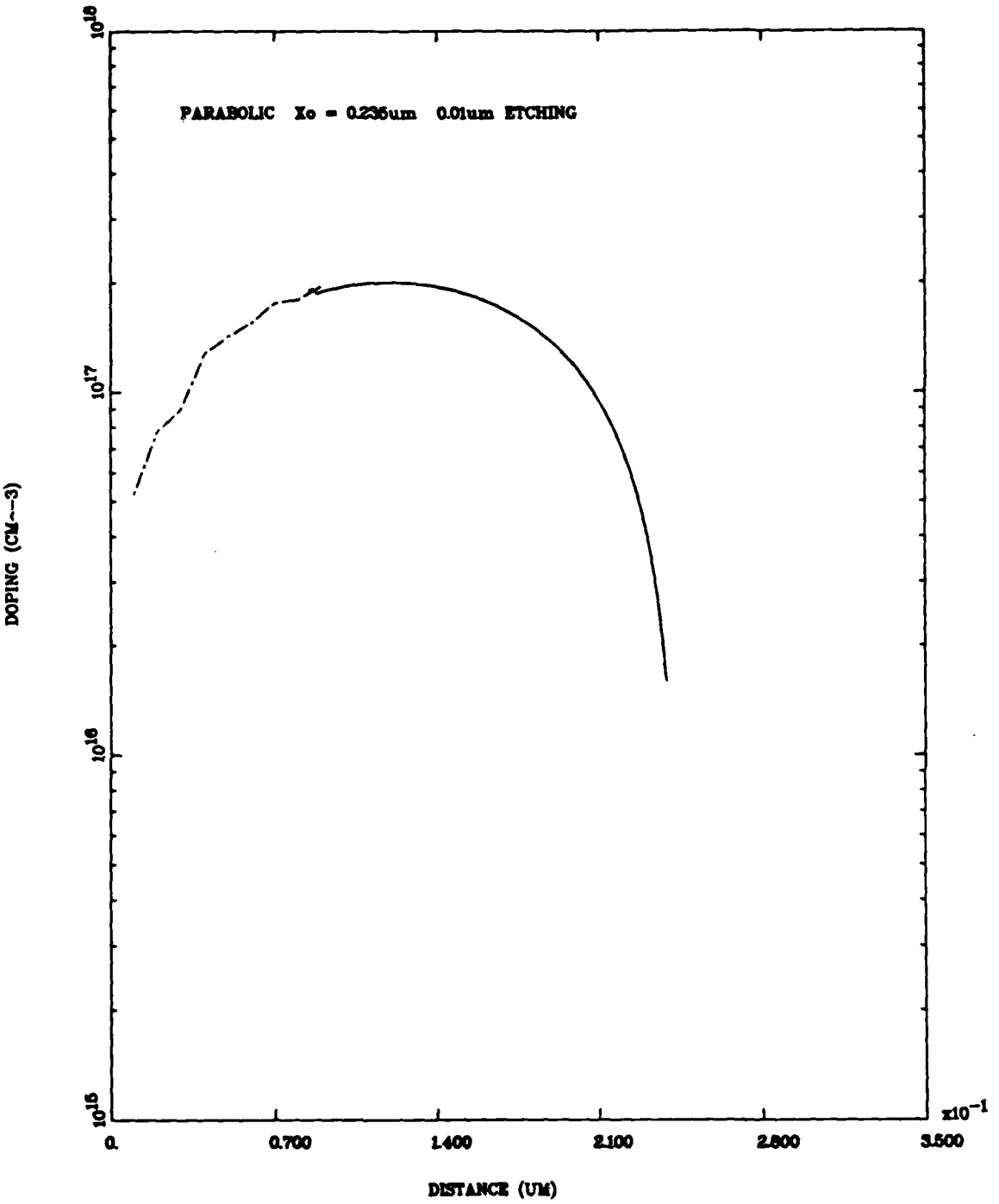

Figure 19. Performance of the Charge Density Moment Method for a Parabolic Profile (Etched Depth Step: 100$\AA$, Reference Point: 0.235μm)

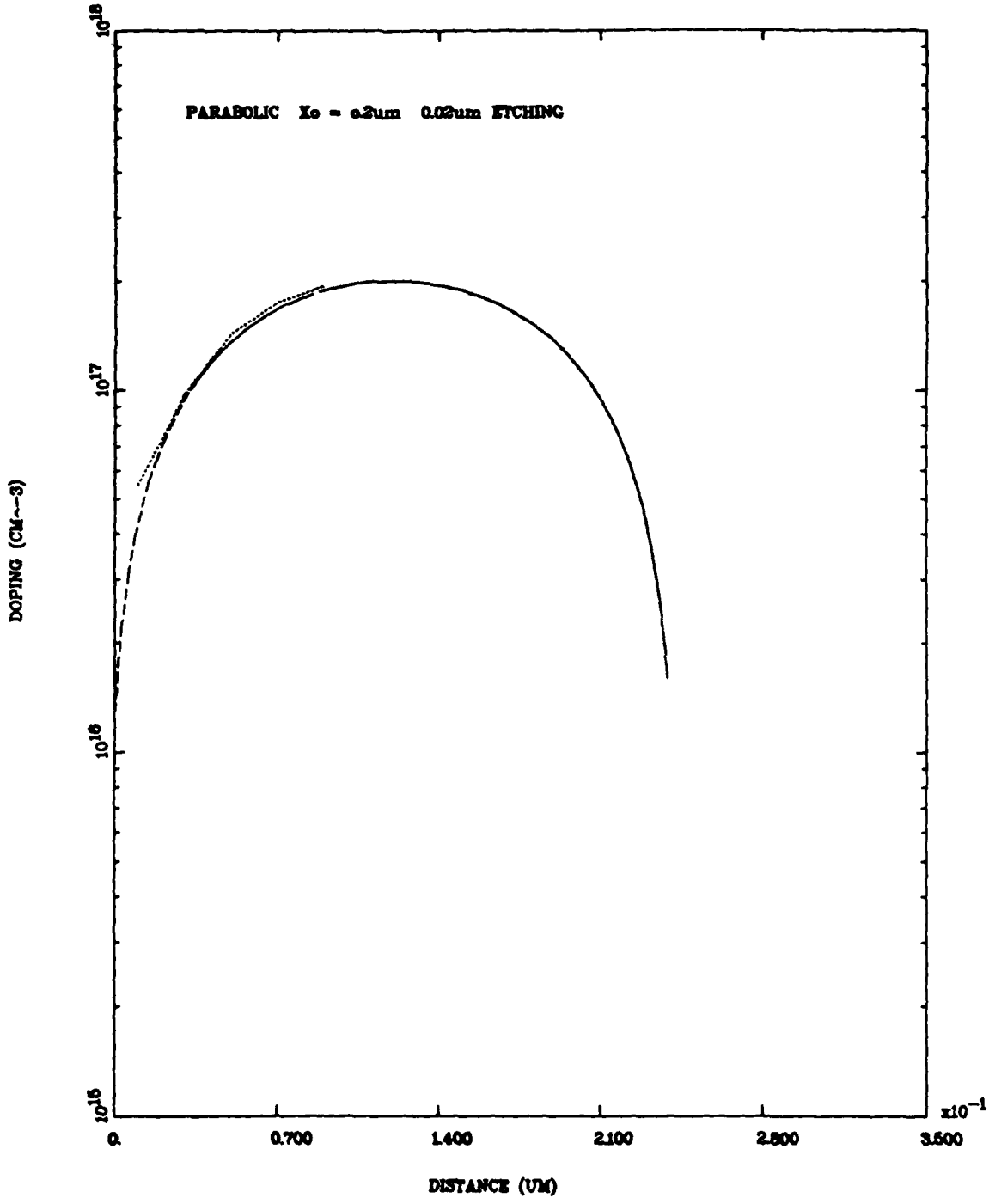

Figure 20. Performance of the Charge Density Moment Method for a Parabolic Profile (Etched Depth Step: 200$\AA$, Reference Point: 0.2μm)

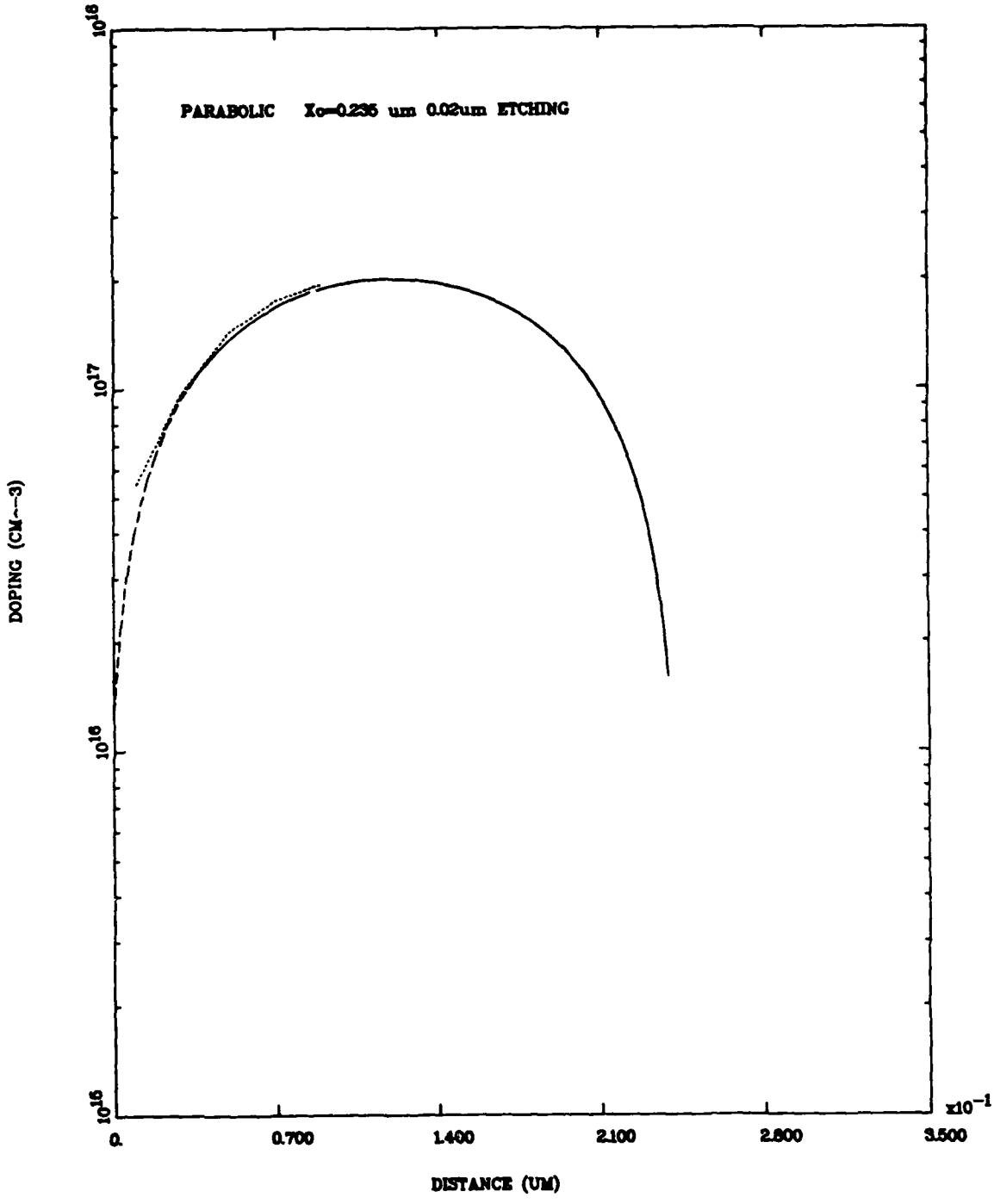

Figure 21. Performance of the Charge Density Moment Method for a Parabolic Profile (Etched Depth Step: 200$\AA$, Reference Point: 0.235μm)

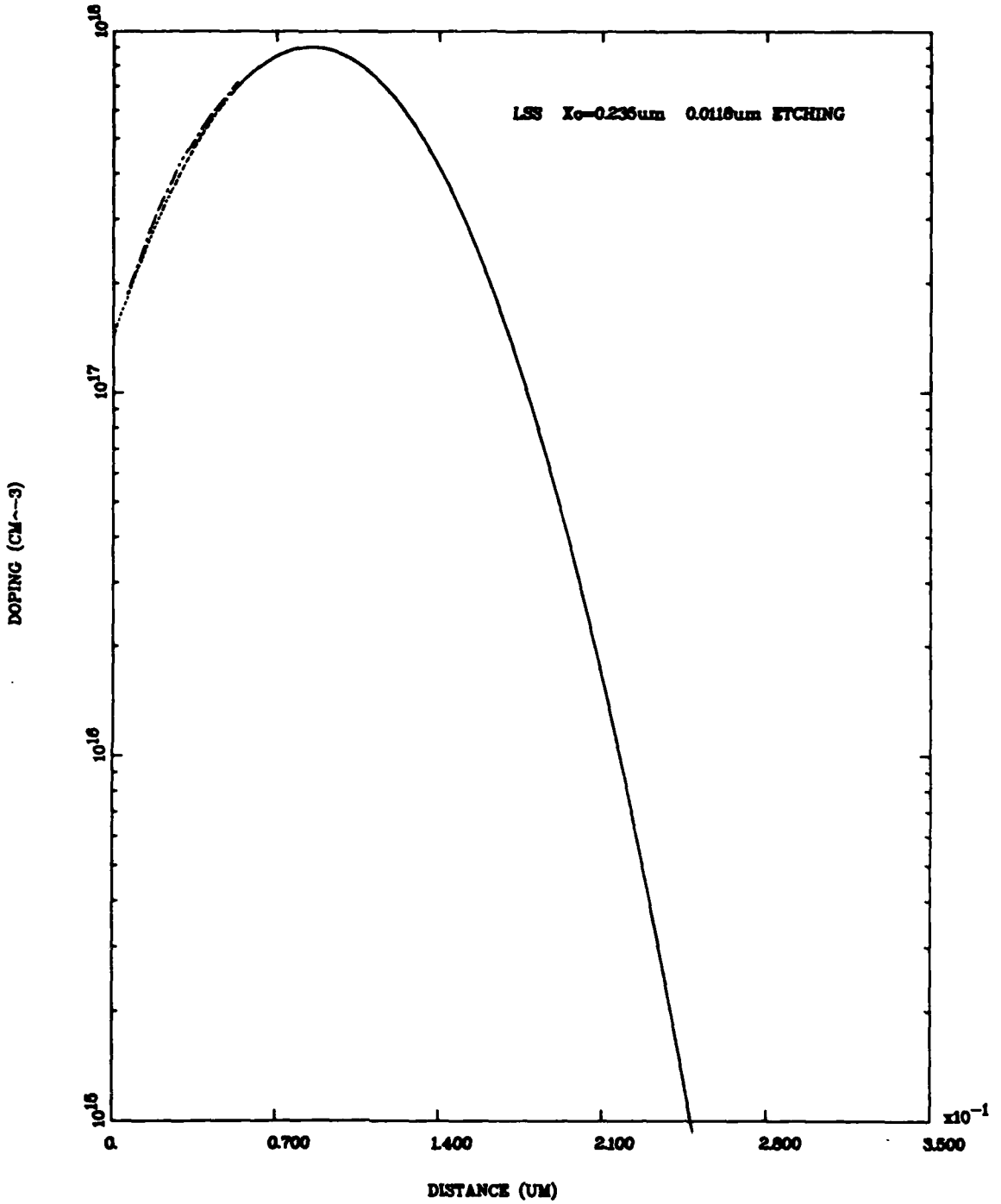

Figure 22. Performance of the Charge Density Moment Method for the LSS Profile for Si implants in GaAs implanted at 100 keV to a Dose of $1 \times 10^{13} cm^{-2}$ (Etched Depth Step: 118Å, Reference Point: 0.235μm)

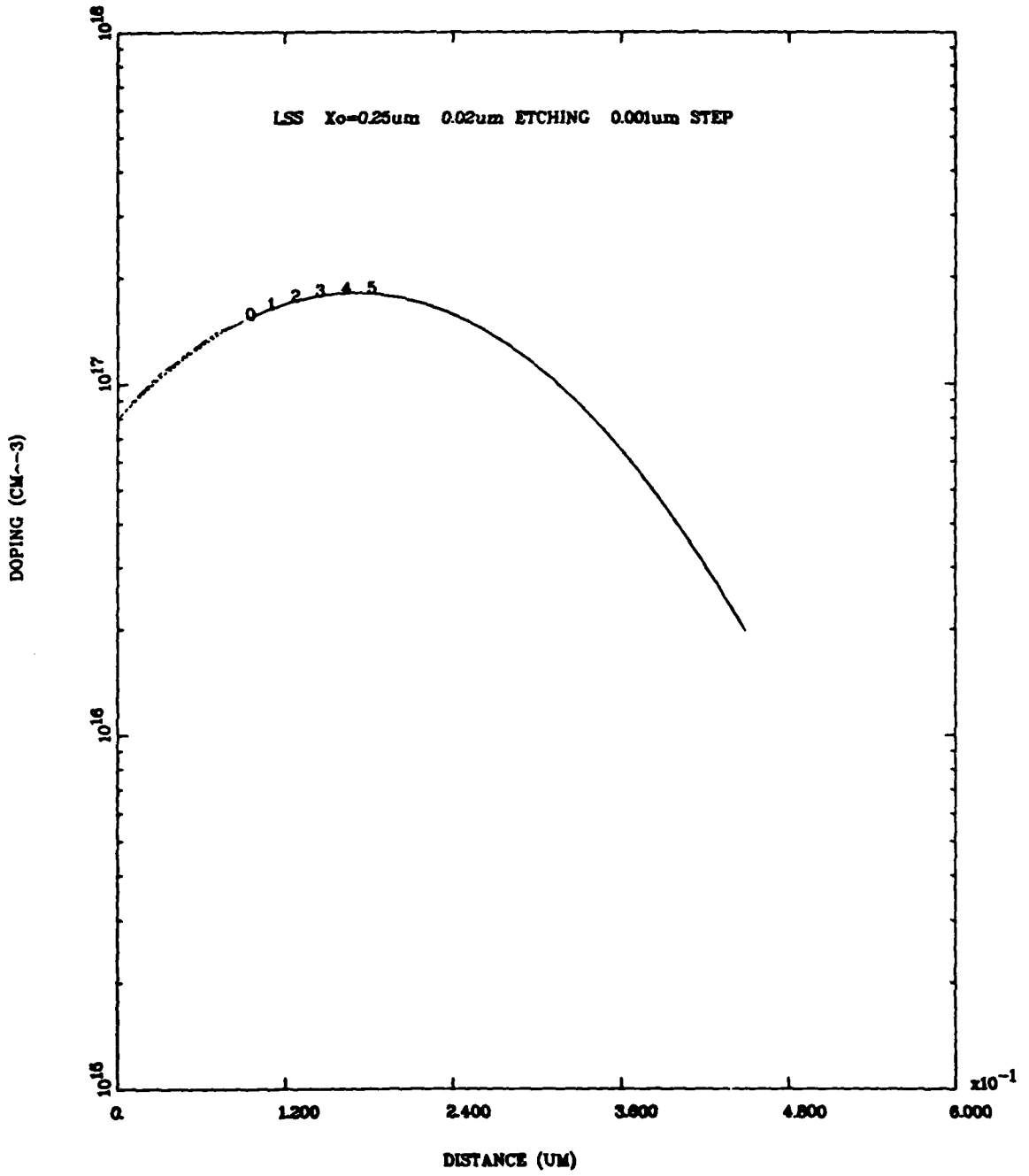

Figure 23. Performance of the Charge Density Moment Method for the LSS Profile for Si implants in GaAs implanted at 100 keV to a Dose of $6 \times 10^{12} cm^{-2}$ (Etched Depth Step: 200$\mathring{A}$, Reference Point: 0.25μm)

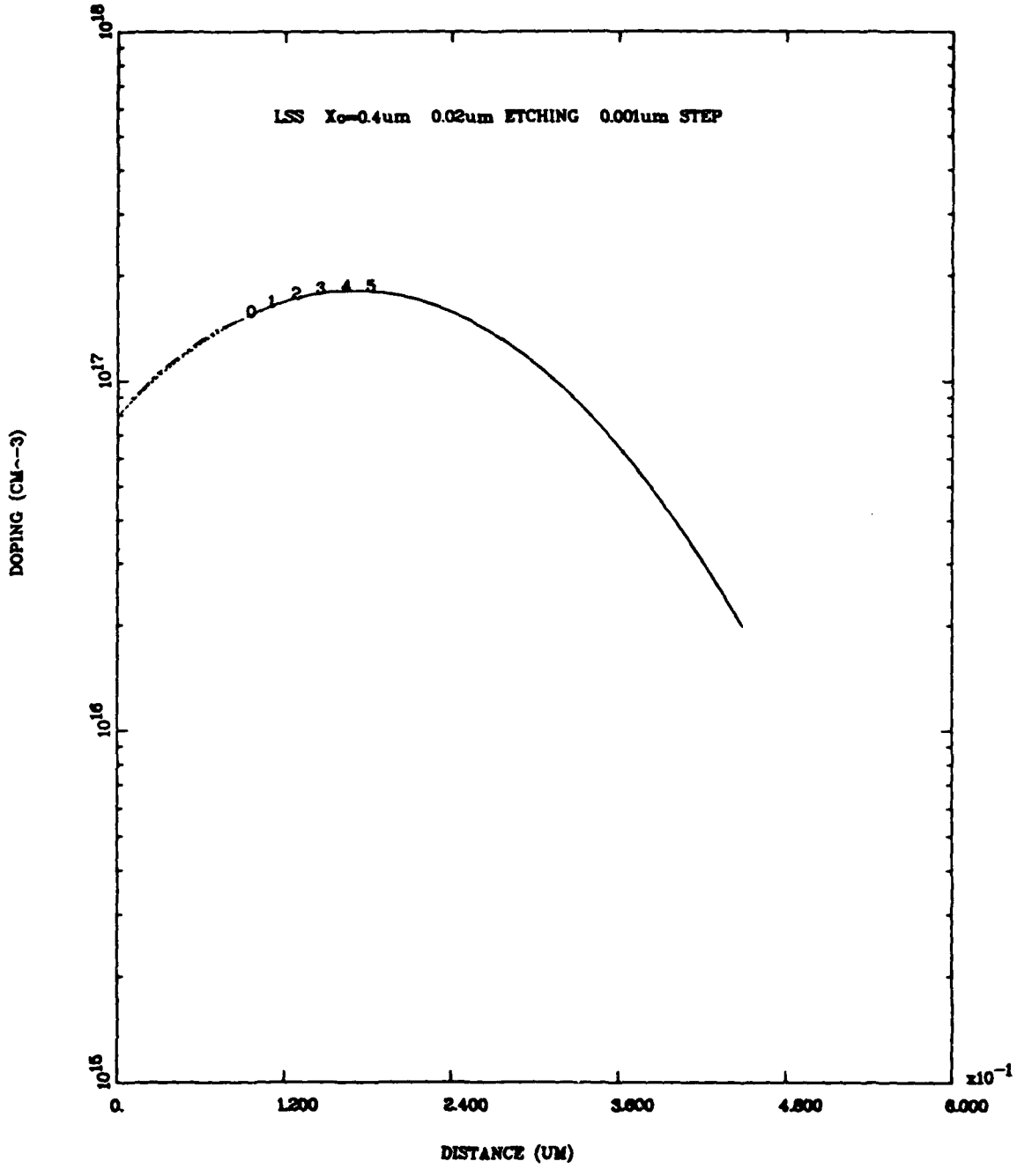

Figure 24. Performance of the Charge Density Moment Method for the LSS Profile for Si implants in GaAs implanted at 100 keV to a Dose of $6\times10^{12}cm^{-2}$ (Etched Depth Step: 200$\AA$, Reference Point: 0.4μm)

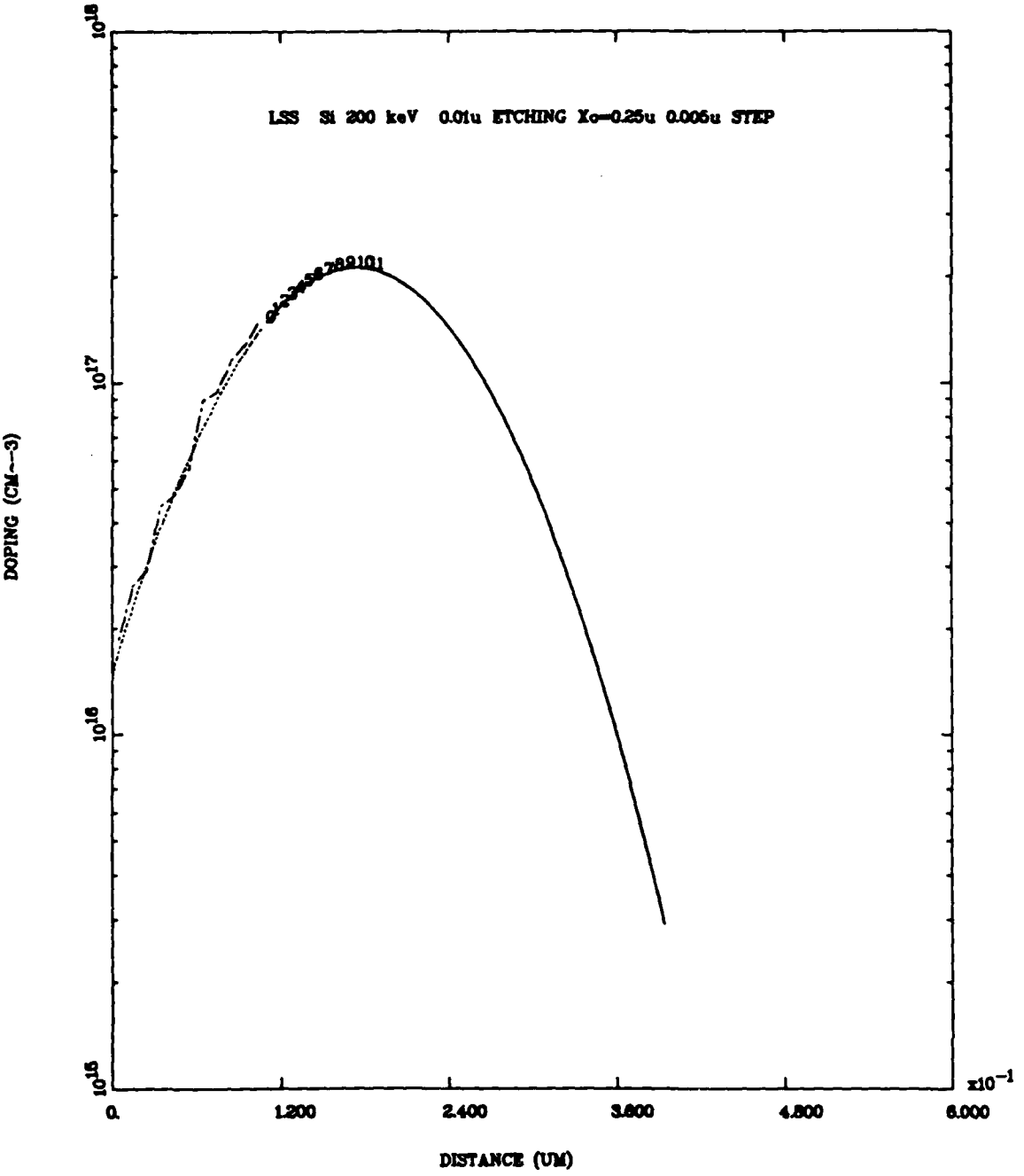

Figure 25. Performance of the Charge Density Moment Method for the LSS Profile for Si implants in GaAs implanted at 200 keV to a Dose of $4 \times 10^{12} cm^{-2}$ (Etched Depth Step: $100\mathring{A}$, Reference Point: 0.25μm)

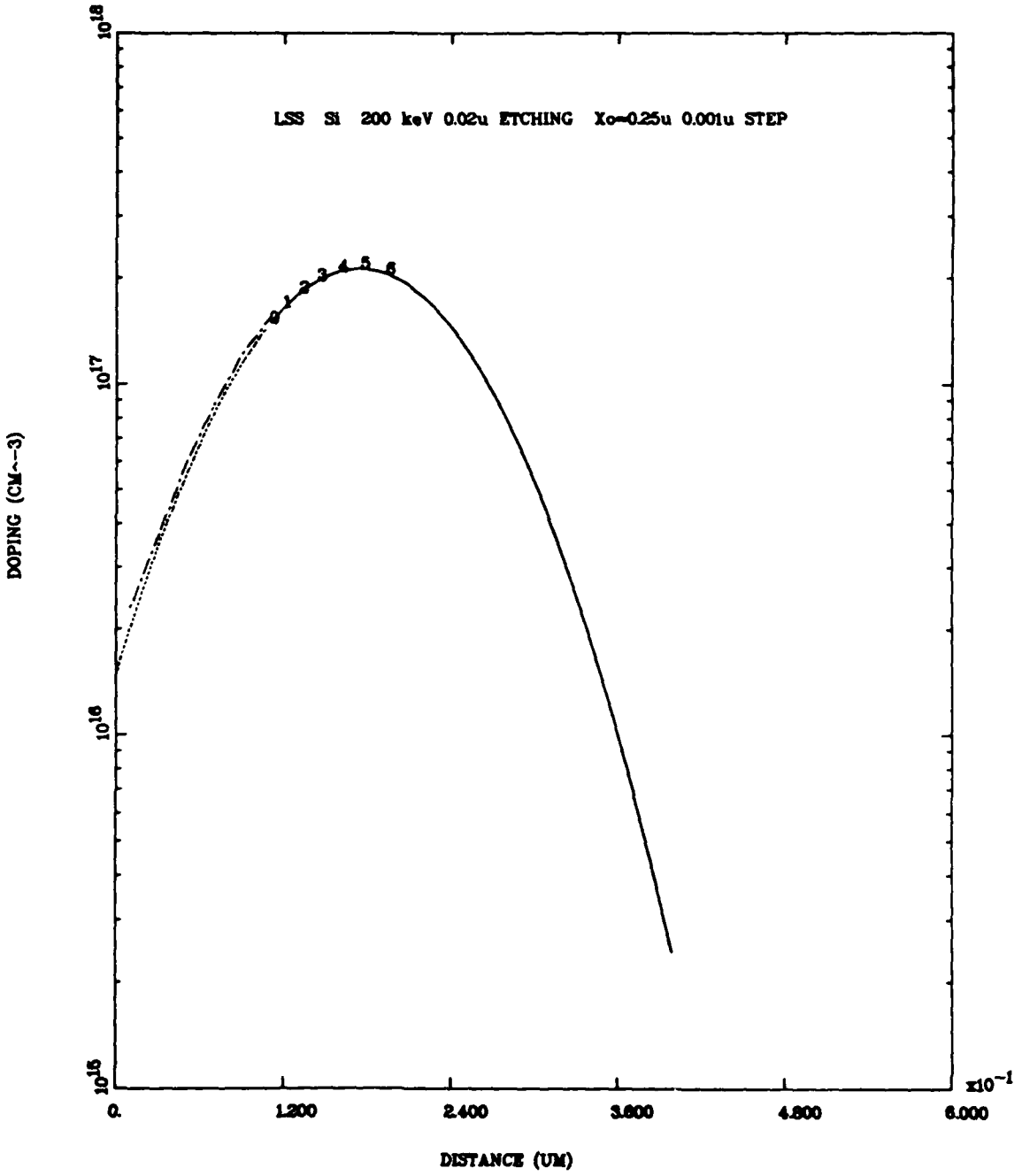

Figure 26. Performance of the Charge Density Moment Method for the LSS Profile for Si implants in GaAs implanted at 200 keV to a Dose of $4\times10^{12}cm^{-2}$ (Etched Depth Step: 200Å, Reference Point: 0.25μm)

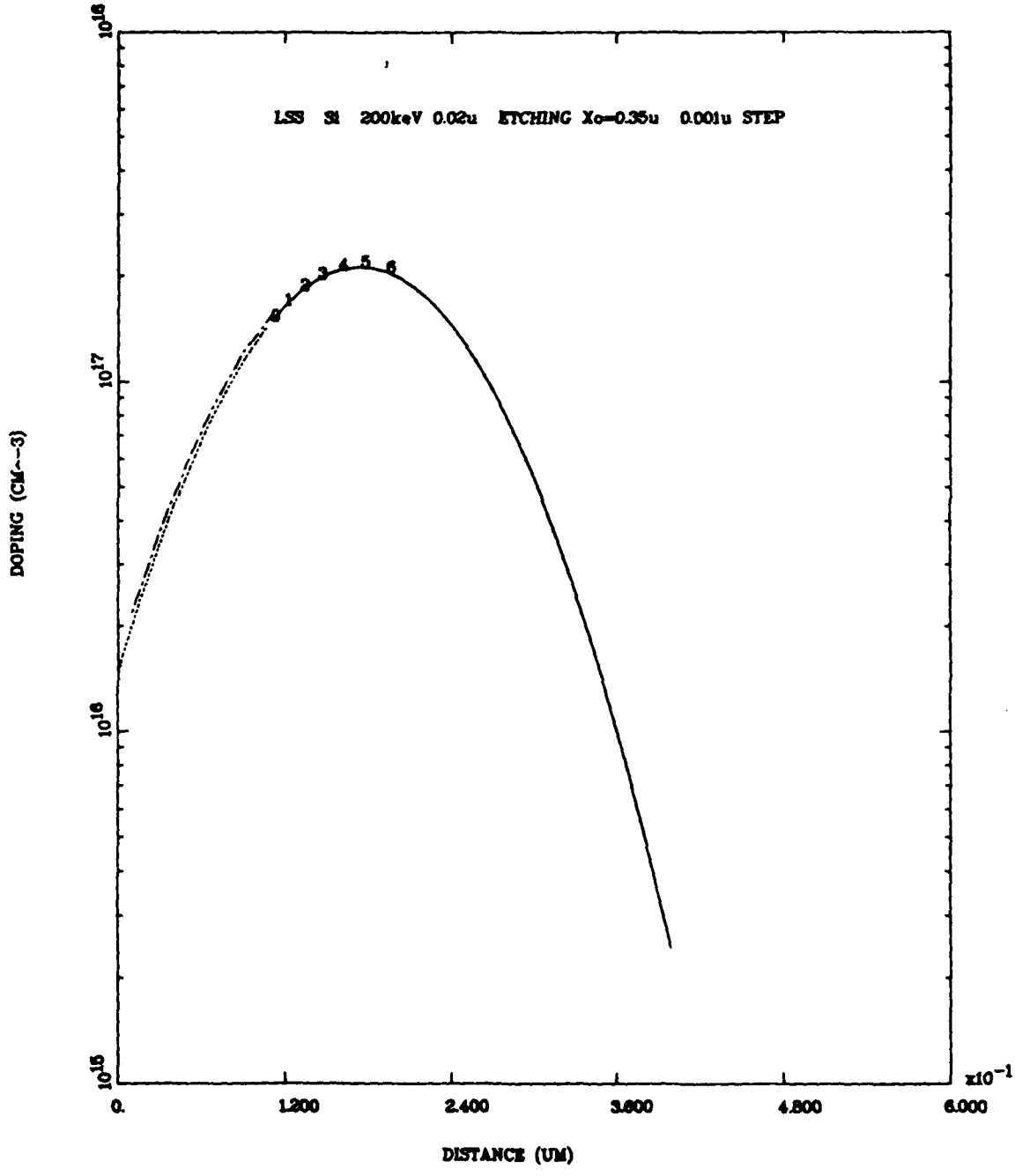

Figure 27. Performance of the Charge Density Moment Method for the LSS Profile for Si implants in GaAs implanted at 200 keV to a Dose of $4 \times 10^{12} cm^{-2}$ (Etched Depth Step: 200Å, Reference Point: 0.35μm)

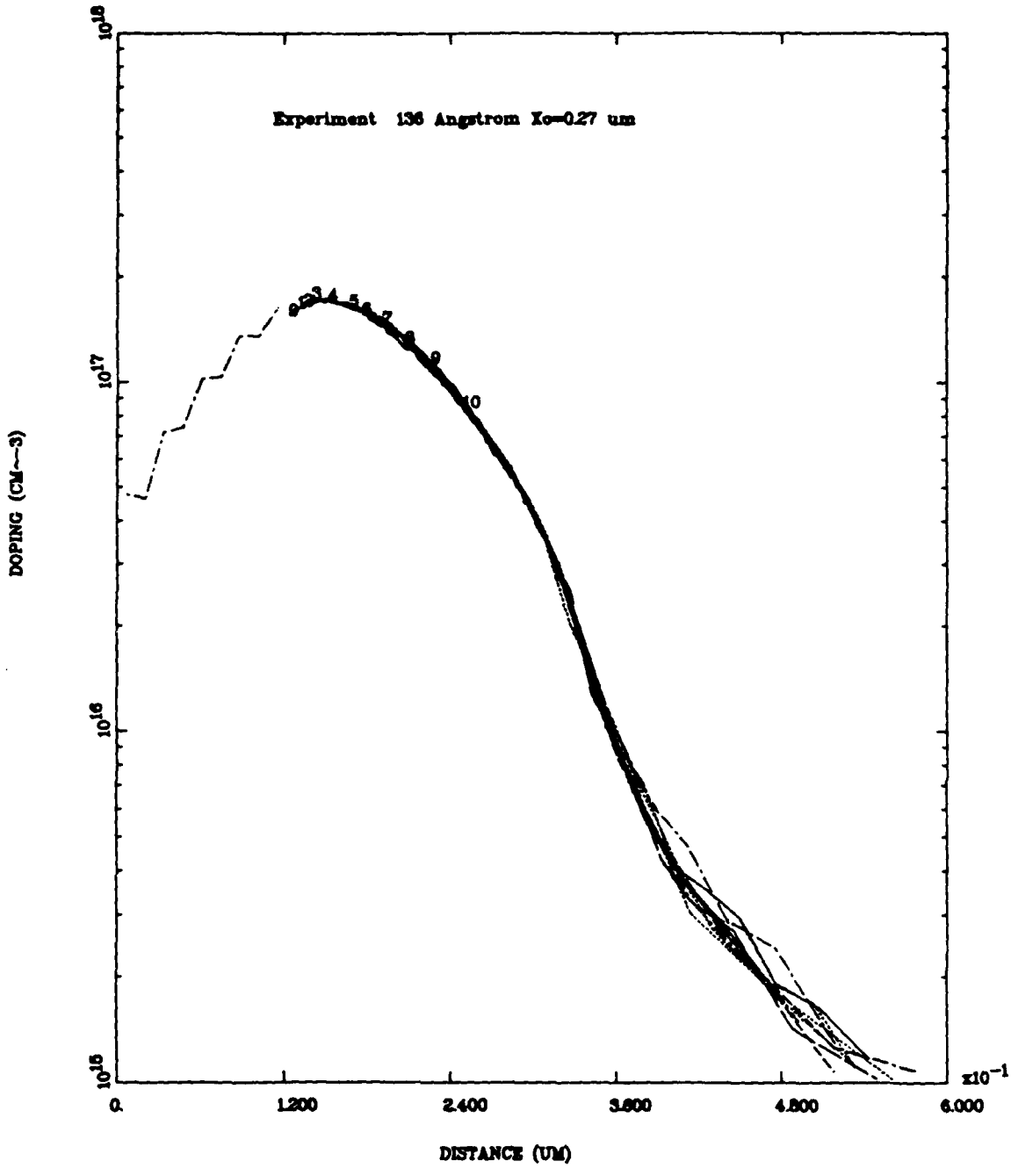

Figure 28. Performance of the Charge Density Moment Method for Si implants in GaAs implanted at 100 keV to a Dose of $8\times10^{12}cm^{-2}$ (Etched Depth Step: 136Å, Reference Point: 0.27μm)

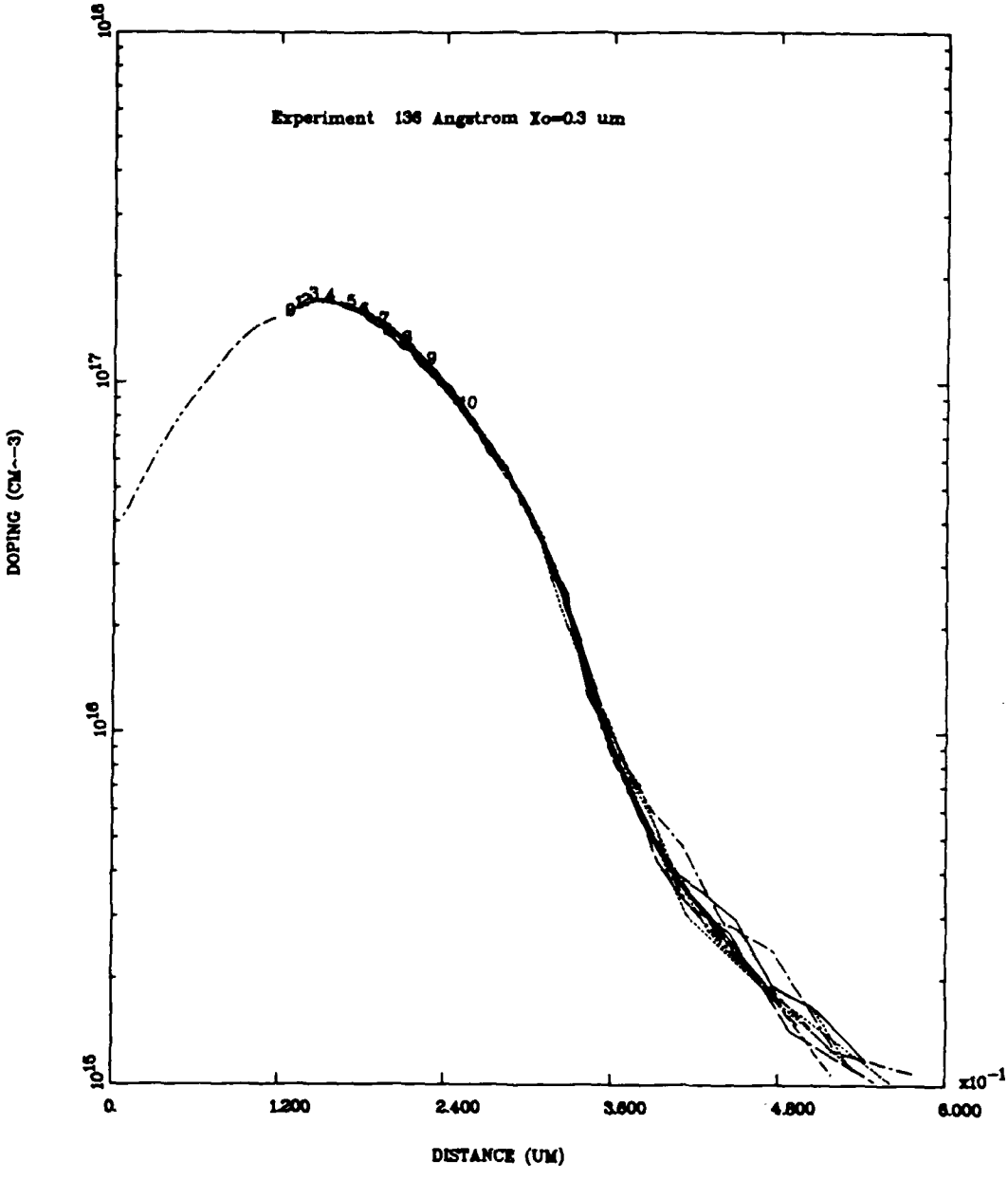

Figure 29. Performance of the Charge Density Moment Method for Si implants in GaAs implanted at 100 keV to a Dose of $8 \times 10^{12} cm^{-2}$ (Etched Depth Step: 136Å, Reference Point: 0.3μm)

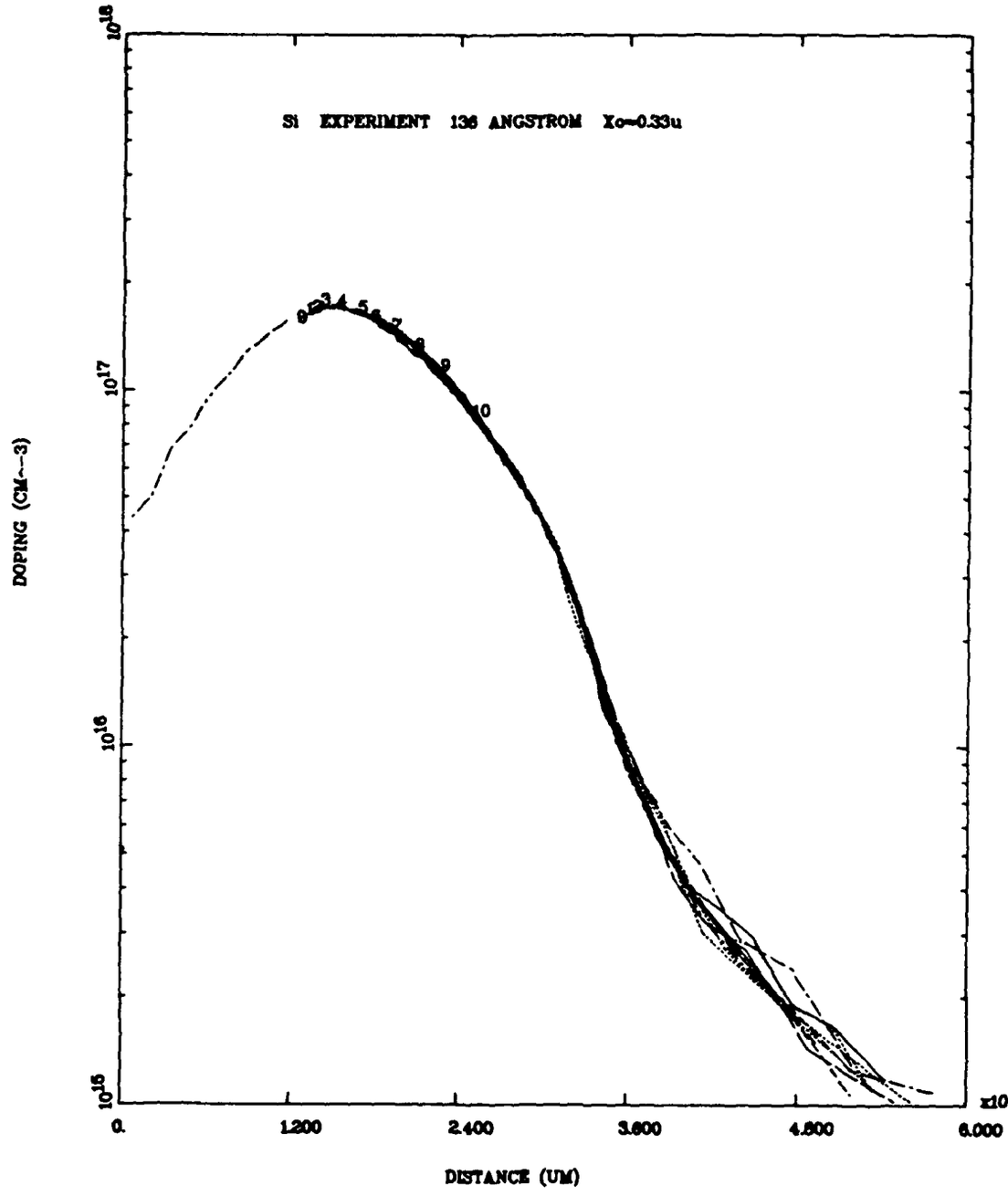

Figure 30. Performance of the Charge Density Moment Method for Si implants in GaAs implanted at 100 keV to a Dose of $8 \times 10^{12} cm^{-2}$ (Etched Depth Step: 118$\mathring{A}$, Reference Point: 0.33μm)

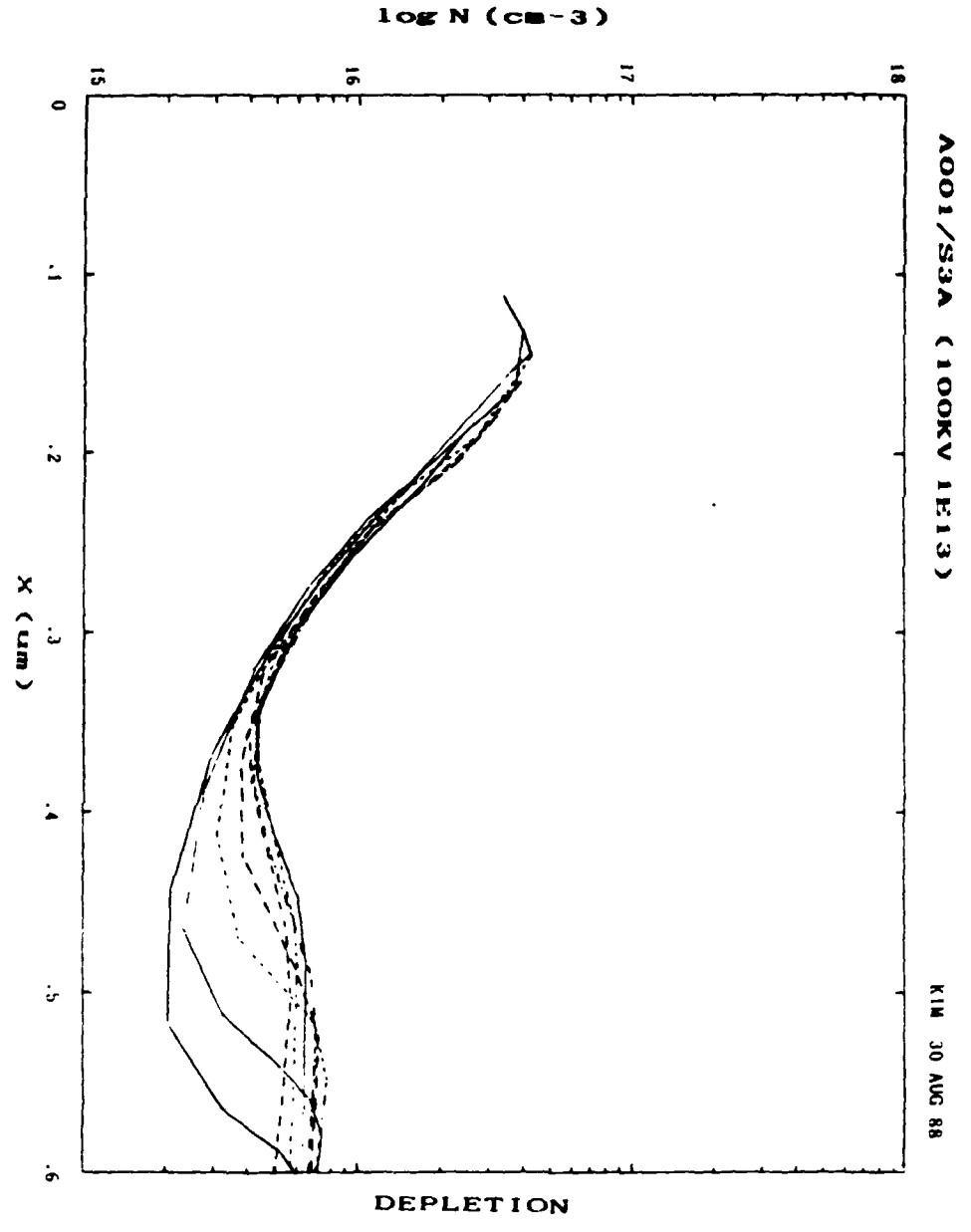

Figure 31. Depletion Profile for Si implants in GaAs implanted at 100 keV to a dose of $1 \times 10^{13} cm^{-2}$ using Polaron Profiler

VII. CONCLUSIONS

The C-V method cannot give carrier distribution informtion within an initial depletion region near the semiconductor surface. Carrier concentration is an important parameter in electronic and opto-electronic device performance. It is therefore essential to develop a method for determining the entire carrier depth profile, right from the semiconductor surface, using the data obtained in a standard C-V depth profile measurement. Methods were developed for finding the carrier concentrations within the initial depletion region of n-type semiconductors. They were the Voltage First Derivative Method, the Voltage Second Derivative Method, and the Charge Density Moment Method. These methods use capacitance-voltage data combined with etching.

In this research, only the Charge Density Moment Method was used. Since this method treats the concentration as uniform between each pair of etch depths, values of the concentrations will be slightly different from the exact values. If the value calculated for the concentration within one etch layer is smaller than the exact value, the calculated value in the next etch layer will compensate by being higher than its exact value. Thus, the concentrations calculated by the Charge Density Moment Method oscillate about the exact profile. Another disadvantage of this method is that it cannot be applied until after etching to the end of the initial depletion region. This means that equation (25) for solving the carrier concentrations within the initial depletion region calculated the carrier concentrations from the depth to the end of initial depletion region of the original unetched surface to backward as shown in Figure 13. The Charge Density Moment Method was also sensitive to experimental C-V data.

The ideal C-V data used a linear, parabolic, and LSS Gaussian functions to find the carrier concentrations within the initial depletion region of n-type semiconductors. For the ideal C-V data, the amount of oscillation varied with the choice

of the etched depth. The profiles calculated by the C-V technique for the different etches overlapped exactly. Also, the calculated carrier concentrations within the depletion region for an etched depth 200 $\AA$ per each layers were very much similar to the true curve. The experimental C-V data covered a Si implants in GaAs implanted at 100 keV to a dose of $1 \times 10^{13}/cm^2$. The profiles for the different etches overlapped only approximately. It showed that this method depends on the reference point and etched depth. A much larger number of finer etches should be performed both within and outside the initial depletion region. Greater accuracy in the measurements of etch thicknesses, voltages, and capacitances would also help. The calculations were rather insensitive to inaccuracies in etch thicknesses, but the thicknesses were measured with an accuracy of about 10%. This means that the accuracy of Charge Density Moment Method depends on the accuracy of experimental C-V data and etched depth. Therefore, for the best results, operator should get rid of experimental errors in generating the experimental C-V data. Also, for reasons of operating program, the Polaron Profiler could not be used in this research.

Finally, the Charge Density Moment Method was very succesful in calculating the carrier concentrations within the initial depletion region of metal-semiconductor contact for the ideal and experimental C-V data.

Appendix A. *Program to Genarate Ideal C-V Data for LSS Gaussian*

```
*
*-------------------------------------------------
*     THIS PROGRAM CREATES VOLTAGE-CAPACITANCE DATA
*           FILE FOR THE LSS GAUSSIAN.
*-------------------------------------------------
*
      REAL VR(0:55,0:1010),C(0:55,0:1010),VRAVG(0:55,0:1010)
     +,XX0(0:55,0:1010),XX1(0:55,0:1010)
      REAL NN,MM
      CHARACTER FILE*4,FIL*3,FILENAME*6
*
*
*
      LU=1
      PRINT*,'ENTER THE FILENAME PREFIX IN 4 CHARACTERS.'
      READ*,FILE
      PRINT*,'THE X STEP SIZE IS .01u/NJ.ENTER NJ.'
      READ*,NJ
      PRINT*,'ENTER THE ETCH DISTANCE IN MICRON:'
      READ*,ED
      PRINT*,'ENTER THE NUMBER OF ETCHES:'
      READ*,NE
      E0=8.854E-14       ! PERMITIVITY OF FREE SPACE
      DC=13.1            !REL. DIELEC.CONST.
      ES=E0*DC
      Q=1.602E-19        ! e:ELECTRON CHARGE
      A=2.04E-3            ! AREA
      B=0.8            !SURFACE BARRIER POTENTIAL
      S=0.0259         !K*T/Q
      ENC=4.352E17


*
*
************************************************************
```

```
*
*     VR(I,J) IS THE JTH VOLTAGE AFTER ITH ETCH.
*     C(I,J) IS THE JTH CAPACITANCE AFTER ITH ETCH.
*
*****************************************************************
*
*
      H=0.01/NJ              ! UNIT: MICRON
      PRINT*,'ENTER THE X MAX: '
      READ*, XM

      DO 20 I=0,NE
      FILENAME=FILE//CHAR(48+INT((I)/10.))//CHAR(48+MOD(I,10))
       OPEN(LU,STATUS='NEW',FILE=FILENAME)
       PRINT*,'   '
       WRITE(LU,*) '  '
       TYPE*,'ENTER THE INITIAL DEPLETION WIDTH W: '
       READ*, W
       TED=I*ED              !TOTAL ETCHED DEPTH
       VR(I,0)=0             ! THE REVERSE BIAS VOLTAGE
       M=(XM-(W+TED))/H
       VBI=B-S*LOG(ENC/(NN(W+TED)*1.E12))   !BUILT-IN POTENTIAL
       PRINT*,'  '
       WRITE(LU,*) '  '
       PRINT*,' '
       WRITE(LU,*) '  '
       PRINT*,'*ETCH NUMBER: ',I
       PRINT*,'*ETCH DEPTH(u): ',TED
       PRINT*,'*INITIAL DEPLETION WIDTH, W(u): ',W
       PRINT*,'*BUILT-IN POTENTIAL VBI :  ',VBI
       WRITE(LU,*) VBI
       WRITE(LU,*) M

*
*
*****************************************************************
*
*
       DDC=MM(W)-MM(W+H)        ! DELTA CAPACITANCE AVERAGE
       C(I,0)=MM(W)+DDC/2       ! INITIAL CAPACITANCE
```

```
      DO 30 J=1,M

       Y=W+(J-1)*H              ! REAL DEPTH FROM THE ETCHED SURFACE
       X=Y+TED                  ! TOTAL DEPTH FROM THE METAL CONTACT
       XX0(I,J)=X
       XX1(I,J)=NN(X)*1.E12          ! CARRIER CONCENTRATION
       XX2=MM(Y)                ! AVERAGE CAPACITANCE
       DCV=-MM(Y)**3/(ES*Q*(A**2)*(NN(X)*1.E12))    ! dC/dV
       C(I,J)=2*MM(Y)-C(I,J-1)
       DC=C(I,J-1)-C(I,J)
       DV=DC/DCV
       VR(I,J)=VR(I,J-1)+DV
       VRAVG(I,J)=(VR(I,J)+VR(I,J-1))/2
       PRINT 501,XX0(I,J),XX1(I,J),VRAVG(I,J)
       WRITE(LU,501) XX0(I,J),XX1(I,J),VRAVG(I,J)
501    FORMAT(2X,F7.5,4X,E12.5,4X,F9.5)
30     CONTINUE
*
*
*****************************************************************
*
*
       CLOSE(LU)
20    CONTINUE
      STOP
      END


*****************************************************************


      REAL FUNCTION NN(X)
       PI=3.1415927
       PH=4.E4
       RP=0.1739
       S=0.0753
       NN=PH/S/SQRT(2.*PI)*EXP(-0.5*((X-RP)/S)**2)
       RETURN
      END


*****************************************************************
```

```
REAL FUNCTION MM(X)   ! C AVERAGE
 EO=8.854E-14
 DC=13.1
 A=2.04E-3
 MM=EO*DC*A/X/1.E-4
 RETURN
END
```

Appendix B. *Program for the Charge Density Moment Method of LSS profile*

```
************************************************************************
*            CHARGE DENSITY MOMENT METHOD
*   This program uses C-V data to determine the doping concentration
*   in the initial depletion region of GaAs. This program uses the
*   LSS curve at the end of the program. This program uses files with
*   names consiting of the first two letter of the month and then the
*   two digit number of the day the data was taken followed by a two
*   digit number of the etch. The files contain the number of average
*   reverse bias voltage(NDATA), the built-in potential(Vbi), the
*   total depth(W(i,j)),the carrier concentration(Nx(i,j)),and then
*   all the average reverse bias voltege.
************************************************************************
      DIMENSION TH(55),TED(55),W(55,1000),V(55)
      DIMENSION DV(55),DVBI(55),NDATA(55),VBI(55),VRAVG(55,1000)
      REAL CN(55),X(55),XP(1000),YP(1000),NX(55,1000),CINT(55)
      REAL NNX,NV,XR(1000),YR(1000)
      COMMON W,VRAVG,NDATA
      CHARACTER FILE*4,CTA*60,FILENAME*6,CID*2
      PRINT*,'ENTER THE FILENAME PREFIX IN 4 CHARACTERS.'
      READ*,FILE
      PRINT*,'ENTER A GRAPH TITLE IN UP TO 60 CHARACTERS.'
      READ*,CTA
      PRINT*,'ENTER THE ETCH RATE IN ANGSTROMS PER MINUTE.'
      READ*,ER
      PRINT*,'ENTER THE TIME PER ETCH IN MINUTES.'
      READ*,T
      PRINT*,'ENTER THE NUMBER OF ETCHS.'
      READ*,NE
      PRINT*,'ENTER THE NUMBER OF ETCHES TO BE USED IN PLOT.'
      READ*,NNE
      PRINT*,'THE X STEP SIZE IS .01U/NJ. ENTER NJ.'
      READ*,NJ
      PRINT*,'ENTER THE COMMON RIGHT EDGE REFERENCE POINT IN UM'
      READ*,XE
      LU=1
```

```
      EO=8.85418E-14          ! PERIMITIVITY OF FREE SPACE
      DC=13.1                 ! REL. DIELEC. CONST
      ES=EO*DC
      Q=1.60218E-19           ! e:ELECTRON CHARGE
*     TH(I) IS THE I-1st ETCH THICKNESS IN cm.
      TH(0+1)=0.
      TED(0+1)=0.
      DO 10 K=1,NE
        I=K+1
        TH(I)=T*ER*1.E-08
10    CONTINUE
      DO 20 K=1,NE
        I=K+1
        TED(I)=TED(I-1)+TH(I)
        PRINT*,TED(I)
20    CONTINUE
      DO 50 K=C,NE
        I=K+1
        FILENAME=FILE//CHAR(48+INT((K)/10.))//CHAR(48+MOD(K,10))
        OPEN(LU,STATUS='OLD',FILE=FILENAME)
        READ(LU,*) VBI(I)
        READ(LU,*) NDATA(I)
          DO 40 J=1,NDATA(I)
            READ(LU,*) W(I,J),NX(I,J),VRAVG(I,J)
40        CONTINUE
        CLOSE(LU)
50    CONTINUE
      OPEN(LU,STATUS='NEW',FILE=FILE//'AC')
*
*     INTERPOLATES TO FIND Vrb(I,XE)
*
      DO 72 K=1,NE+1
        I=K
        NV=0
        J=0
60      J=J+1
        IF (J.GE.NDATA(I)) GOTO 65
        IF (XE.GT.W(I,J)) GOTO 60
        IF (W(I,J)-W(I,J-1).GT.0..AND.J.NE.1) THEN
          NV=(XE-W(I,J-1))*(VRAVG(I,J)-VRAVG(I,J-1))
     +       /(W(I,J)-W(I,J-1))
        ENDIF
```

```
        V(I)=NV+VRAVG(I,J-1)
65      IF (J.GE.NDATA(I)) V(I)=VRAVG(I,NDATA(I))
        PRINT*,'I,J',I,J
72    CONTINUE
      WRITE (LU,*) '* REFERENCE POINT (XO) IS : ',XE
*
*     DO LOOP FINDS POTENTIAL DIFFERENCE BETWEEN ETCH LAYERS WITH
*     COMMON DEPLETION RIGHT EDGE OF XE.
*
      DO 70 K=1,NE
        I=K+1
           DV(I)=ABS(V(I-1)-V(I))
           DVBI(I)=VBI(I-1)-VBI(I)
        PRINT*,'ETCH #, DV,DVBI ARE',I-1,DV(I),DVBI(I)
        WRITE(LU,*) '* ETCH # , DV, DVBI ARE ',I-1,DV(I),DVBI(I)
70    CONTINUE
*
*     DO LOOP FINDS AVERAGE CONCENTRATION BETWEEN ETCH LAYERS.
*
      DO 71 I=1,NE
       CIN=0.
       ST=TED(I+1)*1.E4
       H=(0.01/NJ)
       NK=(XE-ST)/H
       PRINT*,ST,H,NK
       DO 130 K=1,NK
        XCR=K*H+ST
        XCL=(K-1)*H+ST
        CIN=CIN+(H*1.E-4)*((NNX(XCL)+NNX(XCR))*1.E12)/2.
130    CONTINUE
       CINT(I)=CIN
       PRINT*,CINT(I)
71    CONTINUE
      DO 120 M=1,NE
        L=M+1
        GIA=(ES/Q)*(DV(L)+DVBI(L))-(TED(L)-TED(L-1))*CINT(L-1)
        CN(L)=2.*GIA/(TED(L)-TED(L-1))**2
        X(L)=(TED(L)+TED(L-1))/2.*1.E4
        IF (CN(L).GT.1.E18) CN(L)=1.E18
        IF (CN(L).LT.1.E15) CN(L)=1.E15
        PRINT*,'ETCH #,X,N(X) ARE',L-1,X(L),CN(L)
        WRITE(LU,*) '* ETCH #,X,N(X) ARE',L-1,X(L),CN(L)
```

```
        IF (X(L).GT.W(1,1)*1.E4) GOTO 125
120   CONTINUE
125   CLOSE(LU)
*****************************************************************
*     PLOTTING SECTION OF PROGRAM                               *
*        USE THE METALIB SUBROUTINE PROGRAM IN LIBRARY          *
*****************************************************************
      DO 90 K=0,NE
        I=K+1
        FILENAME=FILE//CHAR(48+INT((K)/10.))//CHAR(48+MOD(K,10))
        OPEN(LU,STATUS='OLD',FILE=FILENAME)
        READ(LU,*) VBI(I)
        READ(LU,*) NDATA(I)
          DO 95 J=1,NDATA(I)
             READ(LU,*) W(I,J),NX(I,J),VRAVG(I,J)
95        CONTINUE
        CLOSE(LU)
90    CONTINUE
      XMIN=0.
      XMAX=.6
      YMIN=1.E15
      YMAX=1.E18
92    CONTINUE
      CALL SETPLOT(FILE,15,0,1)
      CALL FRAME
      CALL LABEL(0.45,0.05,'DISTANCE (UM)','H','A')
      CALL LABEL(0.2,0.5,'DOPING (CM^-3)','V','A')
      CALL LABEL(0.3,0.85,CTA,'H','A')
      CALL MAPXY(XMIN,XMAX,YMIN,YMAX,0.25,0.75,0.1,0.92,2,3)
      DO 91 I=1,NNE+1
        DO 100 J=1,NDATA(I)
          XP(J)=W(I,J)
          YP(J)=NX(I,J)
          JC=J
100     CONTINUE
        ISTYLE=MOD(I,5)
        CALL TRACE(XP,YP,JC,ISTYLE)
*       THE ETCH # IS PLACED AT THE START OF EACH CURVE.
         IF ((I-1).GE.10) THEN
           CID=CHAR(48+INT((I-1)/10.))//CHAR(48+MOD(I-1,10))
           ELSE
             CID=CHAR(48+I-1)//' '
```

```
         ENDIF
         XS=XP(1)
         YS=YP(1)
         CALL LABEL(XS,YS,CID,'H','U')
91     CONTINUE
       DO 110 J=2,NNE+1
          IF (X(J).GT.W(1,1)) GOTO 111
          X(J-1)=X(J)
          CN(J-1)=CN(J)
110    CONTINUE
111    CALL TRACE(X,CN,NNE,4)
       HH=W(1,1)/30
       DO 115 J=1,30
         XR(J)=(J-1)*HH
         XRR=XR(J)
         YR(J-1)=NNX(XRR)*1.E12
115    CONTINUE
       CALL TRACE (XR,YR,30,1)
       END
       REAL FUNCTION NNX(X)
         PH=4.E4
         PI=3.1415927
         RP=0.1739
         S=0.00753
         NNX=PH/S/SQRT(2.*PI)*EXP(-0.5*((X-RP)/S)**2)
         RETURN
       END
```

Appendix C. *Program for the Charge Density Moment Method*

```
*****************************************************************
*     CHARGE DENSITY MOMENT METHOD
*   THIS PROGRAM USES C-V DATA TO DETERMINE THE DOPING CONCENTRATION
*   IN THE INITIAL DEPLETION REGION OF GaAs.  THIS PROGRAM USES
*   FILES WITH NAMES CONSISTING OF THE FIRST LETTER OF THE MONTH AND
*   THEN THE TWO DIGIT NUMBER OF THE DAY THE DATA WAS TAKEN FOLLOWED
*   BY A TWO DIGIT NUMBER OF THE ETCH. THE FILES CONTAIN THE NUMBER
*   OF BIAS VOLTAGE(NDATA), THE TOTAL DEPTH(W(I,J)),THE CARRIER
*   CONCENTRATION(NX(I,J)),AND THEN ALL THE BIAS VOLTAGE.
*****************************************************************
      REAL TH(55),TED(55),W(55,1000),V(55),BIAS(55,1000)
      REAL DV(55),DVBI(55),VBI(55),VRAVG(55,1000)
      REAL CN(55),X(55),XP(1000),YP(1000),NX(55,1000),CINT(55)
      REAL NV,D(55,1000),IXE,NXE,ITL,NTL,CIN
      INTEGER NDATA(55)
      CHARACTER FILE*4,CTA*60,FILENAME*6,CID*2
      PRINT*,'ENTER THE FILENAME PREFIX IN 4 CHARACTERS.'
      READ*,FILE
      PRINT*,'ENTER A GRAPH TITLE IN UP TO 60 CHARACTERS.'
      READ*,CTA
      PRINT*,'ENTER THE ETCH RATE IN ANGSTROMS PER MINUTE.'
      READ*,ER
      PRINT*,'ENTER THE TIME PER ETCH IN MINUTES.'
      READ*,T
      PRINT*,'ENTER THE NUMBER OF ETCHS.'
      READ*,NE
      PRINT*,'ENTER THE NUMBER OF ETCHES TO BE USED IN PLOT.'
      READ*,NNE
      PRINT*,'THE X STEP SIZE IS .01U/NJ. ENTER NJ.'
      READ*,NJ
      PRINT*,'ENTER THE COMMON RIGHT EDGE REFERENCE POINT IN UM'
      READ*,XE
      LU=1
      EO=8.85418E-14
      DC=13.1
      ES=EO*DC
      Q=1.60218E-19
```

```
      B=0.8
      S=0.0259
      ENC=4.352E17
*
*   EO IS A PERMITIVITY OF FREE SPACE.
*   DC IS A RELATIVE DIELECTRIC CONSTANT.
*   Q IS A ELECTRON CHARGE.
*   B IS A SURFACE BARRIER POTENTIAL.
*
*   TH(I) IS THE I-1st ETCH THICKNESS IN cm.
*
      TH(0+1)=0.
      TED(0+1)=0.
      DO 10 K=1,NE
        I=K+1
        TH(I)=T*ER*1.E-08
10    CONTINUE
      DO 20 K=1,NE
        I=K+1
        TED(I)=TED(I-1)+TH(I)
        PRINT*,TED(I)
20    CONTINUE
      DO 50 K=0,NE
        I=K+1
        FILENAME=FILE//CHAR(48+INT((K)/10.))//CHAR(48+MOD(K,10))
        OPEN(LU,STATUS='OLD',FILE=FILENAME)
        READ(LU,*) NDATA(I)
          DO 40 J=1,NDATA(I)
            READ(LU,*) W(I,J),NX(I,J),BIAS(I,J),D(I,J)
40        CONTINUE
        CLOSE(LU)
50    CONTINUE
      DO 55 I=1,NE+1
        VBI(I)=B-S*LOG(ENC/NX(I,1))
        DO 56 J=1,NDATA(I)
          VRAVG(I,J)=(BIAS(I,J)+BIAS(I,J+1))/2
56      CONTINUE
55    CONTINUE
      OPEN(LU,STATUS='NEW',FILE=FILE//'AC')
*
*     INTERPOLATES TO FIND Vrb(I,XE)
*
```

```
      DO 72 K=1,NE+1
        I=K
        NV=0
        J=0
60      J=J+1
        IF (J.GE.NDATA(I)) GOTO 65
        IF (XE.GT.W(I,J)) GOTO 60
        IF (W(I,J)-W(I,J-1).GT.0..AND.J.NE.1) THEN
          NV=(XE-W(I,J-1))*(VRAVG(I,J)-VRAVG(I,J-1))
     +       /(W(I,J)-W(I,J-1))
        ENDIF
        V(I)=NV+VRAVG(I,J-1)
65      IF (J.GE.NDATA(I)) V(I)=VRAVG(I,NDATA(I))
        PRINT*,'I,J',I,J
        WRITE(LU,*) I,J
72    CONTINUE
      WRITE (LU,*) '* REFERENCE POINT (XO) IS : ',XE
*
*     DO LOOP FINDS POTENTIAL DIFFERENCE BETWEEN ETCH LAYERS
*     WITH COMMON DEPLETION RIGHT EDGE OF XE.
*
      DO 70 K=1,NE
        I=K+1
          DV(I)=ABS(V(I-1)-V(I))
          DVBI(I)=VBI(I-1)-VBI(I)
        PRINT*,'ETCH #, DV,DVBI ARE',I-1,DV(I),DVBI(I)
        WRITE(LU,*) '* ETCH # , DV, DVBI ARE ',I-1,DV(I),DVBI(I)
70    CONTINUE
*
*     DO LOOP FINDS AVERAGE CONCENTRATION BETWEEN ETCH LAYERS.
*
      NXE=0
      J=0
73    J=J+1
      IF(XE.GT.W(2,J)) GOTO 73
      IF(W(2,J)-W(2,J-1).GT.0..AND.J.NE.1) THEN
        NXE=(XE-W(2,J-1))*(NX(2,J)-NX(2,J-1))/(W(2,J)-W(2,J-1))
      ENDIF
      IXE=NXE+NX(2,J-1)
      WRITE(LU,*) 'CONCENTRATION OF XE IS',IXE
      DO 120 M=NE,1,-1
        L=M+1
```

```
        X(L)=(TED(L)+TED(L-1))/2.*1.E4
        IF(TED(L)*1.E4.GE.W(2,1)) THEN
           ITL=0
           J=0
121        J=J+1
           IF(J.GE.NDATA(2)) GOTO 122
           IF(TED(L)*1.E4.GT.W(2,J)) GOTO 121
           IF(W(2,J)-W(2,J-1).GT.0..AND.J.NE.1) THEN
               ITL=(TED(L)*1.E4-W(2,J-1))*(NX(2,J)-NX(2,J-1))
     +              /(W(2,J)-W(2,J-1))
           ENDIF
           NTL=ITL+NX(2,J-1)
122        IF(J.GE.NDATA(2)) NTL=NX(2,NDATA(2))
           CIN=((W(2,J)*1.E-4)-TED(L))*(NTL+NX(2,J))/2
123        J=J+1
           CIN=CIN+((W(2,J)-W(2,J-1))*1.E-4)
     +           *(NX(2,J)+NX(2,J-1))/2
           IF(W(2,J).LT.XE) GOTO 123
           CINT(L)=CIN+(XE-W(2,J-1))*1.E-4*(IXE+NX(2,J-1))/2
           GIA=(ES/Q)*(DV(L)+DVBI(L))-(TED(L)-TED(L-1))*CINT(L)
           CN(L)=2.*GIA/(TED(L)-TED(L-1))**2
           IF(CN(L).GT.1.E18) CN(L)=1.E18
           IF(CN(L).LT.1.E15) CN(L)=1.E15
           WRITE(LU,*) 'ETCH #,X,N(X),SUM ARE',L-1,X(L),CN(L),CINT(L)
        ELSE
        CINT(L)=CINT(L+1)+CN(L+1)*(TED(L)-TED(L-1))
        GIA=(ES/Q)*(DV(L)+DVBI(L))-(TED(L)-TED(L-1))*CINT(L)
        CN(L)=2.*GIA/(TED(L)-TED(L-1))**2
        IF (CN(L).GT.1.E18) CN(L)=1.E18
        IF (CN(L).LT.1.E15) CN(L)=1.E15
        PRINT*,'ETCH #,X,N(X) ARE',L-1,X(L),CN(L)
        WRITE(LU,*) '* ETCH #,X,N(X),SUM ARE',L-1,X(L),CN(L),CINT(L)
        ENDIF
        IF(X(L).GT.W(1,1)*1.E4)  GOTO 125
120   CONTINUE
125   CLOSE(LU)
*****************************************************************
*     PLOTTING SECTION OF PROGRAM (USING METALIB)
*****************************************************************
      DO 90 K=0,NE
        I=K+1
        FILENAME=FILE//CHAR(48+INT((K)/10.))//CHAR(48+MOD(K,10))
```

```
        OPEN(LU,STATUS='OLD',FILE=FILENAME)
        READ(LU,*) NDATA(I)
          DO 95 J=1,NDATA(I)
             READ(LU,*) W(I,J),NX(I,J),BIAS(I,J),D(I,J)
95        CONTINUE
        CLOSE(LU)
90    CONTINUE
      XMIN=0.
      XMAX=.6
      YMIN=1.E15
      YMAX=1.E18
92    CONTINUE
      CALL SETPLOT(FILE,15,0,1)
      CALL FRAME
      CALL LABEL(0.45,0.05,'DISTANCE (UM)','H','A')
      CALL LABEL(0.2,0.5,'DOPING (CM^-3)','V','A')
      CALL LABEL(0.35,0.85,CTA,'H','A')
      CALL MAPXY(XMIN,XMAX,YMIN,YMAX,0.25,0.75,0.1,0.92,2,3)
      DO 91 I=1,NNE+1
        DO 100 J=1,NDATA(I)
         IF(W(I,J).LE.XMAX.AND.NX(I,J).GE.YMIN) THEN
           XP(J)=W(I,J)
           YP(J)=NX(I,J)
           JC=J
           ELSE
             GOTO 93
         ENDIF
100     CONTINUE
93      ISTYLE=MOD(I,5)
        CALL TRACE (XP,YP,JC,ISTYLE)
*
*        THE ETCH # IS PLACED AT THE START OF EACH CURVE.
*
         IF ((I-1).GE.10) THEN
           CID =CHAR(48+INT((I-1)/10.))//CHAR(48+MOD(I-1,10))
           ELSE
             CID=CHAR(48+I-1)//'  '
         ENDIF
         XS=XP(1)
         YS=YP(1)
         CALL LABEL(XS,YS,CID,'H','U')
91    CONTINUE
```

```
      DO 110 J=2,NNE+1
          IF (X(J).GT.W(1,1)) GOTO 111
          X(J-1)=X(J)
          CN(J-1)=CN(J)
110   CONTINUE
111   CALL TRACE(X,CN,NNE,4)
      END
```

Appendix D. *Program to Calculate the Depletion Widths for a LSS Gaussian Distribution*

This computer program was written by David W. Elsaesser, Capt. USAF to calculate the depletion widths for a gaussian distribution.

```
  PROGRAM DWGAUSS
*****************************************************************
*       THIS PROGRAM CALCULATES THE DEPLETION WIDTHS FOR
*       A GUASSIAN DISTRIBUTION
*****************************************************************
         DIMENSION XS(0:200),W(0:200),X(200),COEFM(80),COEFR(80)
         DIMENSION COEF(80),COEFD(80)
         REAL N(200)
         CHARACTER*1 ANS
         CHARACTER*50 CAR(10)
         FNMEAS(Y)=RNGM*EXP(-(((Y-RPM)/SIGM)**2)/2)
         CAR(1)= '(''$  ENTER REAL DOSE, PROJ RANGE, SIGMA: '')'
         CAR(2)= '(''$     TYPE C TO CONTINUE OR Q TO QUIT: '')'
         CAR(3)= '(''$           ORDER OF FITTING MEASURED: '')'
         CAR(4)= '(''$               ORDER OF FITTING REAL: '')'
         WRITE(*,CAR(1))
         READ*,DOSER,RPR,SIGR
         RNGR=DOSER*10000./SIGR/2.5066283
         TYPE*,RNGR
         COEFR(1)=ALOG(RNGR)-(RPR**2)/2./SIGR**2
         COEFR(2)=RPR/SIGR**2
         COEFR(3)=-1./2./SIGR**2
         WRITE(*,CAR(3))
         READ*,NOM
         WRITE(*,CAR(4))
         READ*,NOR
         CALL NDEPWID(2,COEFR,DOSER,SIGR,RPR,H0,NVP,W)
         CALL DEPWID(2,COEFR,DOSER,SIGR,RPR,H0,NVP,W)
         STOP
         END
         SUBROUTINE DEPWID(NO,COEF,DOSE,SIG,RP,H1,NVP,W)
*
```

```
*     THIS PROGRAM FINDS THE DEPLETIONS WIDTHS BY SELF-CONSISTENTLY
*     AVERAGING THE DOPING PROFILE WITHIN THE DEPLETION REGION AND
*     THEN CALCULATING THE DEPLETION WIDTH ASSUMING A CONSTANT DOPING
*     PROFILE
*
          REAL N,NM(0:100),NSC(0:50000),H0,H1
          DIMENSION W(0:200),COEF(80)
          DIMENSION XM(0:200)
          FNVBS(N)= .8-(0.674-.0259*ASINH(N/2/2.17E6))
          FNW(N)=3.8051E7*((VBS-ALPH*.0259)/N)**.5
          WRITE(*,'($,36A)')' INCLUDE MAJORITY CARRIER (0 OR 1): '
          READ(*,*)ALPH
          NINT=50000
          F1=3.
          NWS=70
          XMAX=RP+SIG*F1
          H0=XMAX/NINT
          H1=XMAX/NWS
          NSC(0)=0
*
*         COMPUTE SHEET CONCENTRATIONS
*
          DO 10 J=1,NINT
          NSC(J)=NSC(J-1)+FN(NO,COEF,(J-.5)*H0)*H0/10000
10        CONTINUE
          W(0)=.07
*
*         CALCULATING W'S
*
          DO 50 J=0,100
          I=0
          IF (J.NE.0) W(J)=W(J-1)
35        X=(W(J)+J*H1)/H0
          K=INT(X)
          DX=X-K
          Y=J*H1/H0
          L=INT(Y)
          DL=Y-L
           IF (X.GT.NINT) THEN
            NVP=J-1
            GOTO 100
           ENDIF
```

```
      N=(NSC(K)+(NSC(K+1)-NSC(K))*DK-NSC(L)-(NSC(L+1)-NSC(L))*DL)*
     1            10000/W(J)
      VBS=FNVBS(N)
      WF=FNW(N)
      I=I+1
      IF (I.GT.100) THEN
       TYPE*,'INPUT WF: '
       READ*,WF
       I=1
      ENDIF
      IF (ABS(W(J)-WF).GT.1E-5) THEN
       W(J)=(W(J)+WF)/2
       GOTO 35
      ENDIF
       TYPE*,J,J*H1,W(J)
50    CONTINUE
      NVP=70
100   CONTINUE
      DO 150 J=1,NVP
      X=(W(J)+J*H1)/H0
      K=INT(X)
      DX=X-K
      Y=(W(J-1)+(J-1)*H1)/H0
      L=INT(Y)
      DL=Y-L
      NM(J)=(NSC(K)+(NSC(K+1)-NSC(K))*DK-NSC(L)-(NSC(L+1)-NSC(L))
     1          *DL)*10000/H1
      XM(J)=(J-.5)*H1
150   CONTINUE
      OPEN(UNIT=10,STATUS='NEW',FILE='AVGDW.DAT')
      WRITE(10,*)NVP+1,2
      DO 210 J=0,NVP
      WRITE(10,*)J*H1,W(J)
210   CONTINUE
      CLOSE(10)
      RETURN
      END
      SUBROUTINE NDEPWID(NO,COEF,DOSE,SIG,RP,H0,NVP,W)
*
*     THIS PROGRAM FINDS THE DEPLETIONS WIDTHS BY SOLVING POISSON'S
*     EQUATION.  THE EQUATION IS SOLVED FROM A GUESS OF THE VALUE OF
*     THE DEPLETION WIDTH.  THE EQUATION IS SOLVED BACKWARDS TOWARDS
```

```
*     THE SURFACE UNTIL THE BUILT IN POTENTIAL IS OBTAINED.
*
      REAL N,NSC(0:2000),H0
      DIMENSION W(0:200),X(0:200),V(0:10001),COEF(80)
      REAL NM(0:100)
      FNVBS(N)= 0.674-.0259*ASINH(N/2./2.17E6)
      FNW(N)=3.8051E7*((VBS-.0259)/N)**.5
      FNV(J)=2*V(J+1)-V(J+2)+(H**2)*1.381E-15*
      NP=500
      F1=.75
      RES=.00002
      NVP=50
      WRITE(*, '($,''    X MAX: '')')
      READ*, XMAX
      H0=XMAX/50
      DO 10 I=0,50
      EW=I*H0
      IF (I.EQ.0.OR.I.EQ.1) THEN
       A=0
       B=.2
       WT=.05
      ELSE
       A=.75*W(I-1)
       B=1.5*ABS(W(I-1)-W(I-2))+1.1*W(I-1)
       WT=W(I-1)
      ENDIF
      NBC=0         !NUMBER OF B CHANGES
15    continue !TYPE*,'WT: ',WT
      H=WT/NP
      V(NP)=FNVBS(FN(NO,COEF,NP*H+EW))
      V(NP+1)=V(NP)   !  FNVBS(FN(NO,COEF,(NP+1)*H+EW))
      DO 20 J=NP-1,0,-1
      V(J)=FNV(J)
      IF (V(J).GT..8)THEN
       B=WT
       NBC=1
       GOTO 45
      ENDIF
20    CONTINUE
40    A=WT                    !V(0) < .8
45    WP=WT
      WT=(A+B)/2
```

```
            IF (ABS(WT-WP).LT.RES)THEN
             IF (NBC.EQ.0) THEN
              NVP=I-1
              GOTO 30
             ENDIF
             W(I)=WT
             TYPE*,I,EW+WT,W(I)
             GOTO 10
            ELSE
             GOTO 15
            ENDIF
10          CONTINUE
30          NVP=NVP-1
            OPEN(UNIT=10,STATUS='NEW',FILE='DEPW.DAT')
            WRITE(10,*)NVP+1,2
            DO 210 J=0,NVP
            X(J)=J*H0
            WRITE(10,*)X(J),W(J)
210         CONTINUE
            WRITE(10,*)RNG,RP,SIG
            CLOSE(10)
            RETURN
            END
            FUNCTION ASINH(X)
*
*       TAKE THE ARC HYPERBOLIC SINE OF X
*
            ASINH=LOG(X+(X**2+1)**.5)
            RETURN
            END
            FUNCTION FN(NO,COEF,X)
*
*       CALCULATE THE DOPING CONCENTRATION OF THE
*       FORM N(X)=EXP[ SUM(0-NO) COEF(I)*X**I]
*
            DIMENSION COEF(80)
            SUM=COEF(1)
            DO 10 I=2,NO+1
            SUM=SUM+COEF(I)*X**(I-1)
10          CONTINUE
            FN=EXP(SUM)
            RETURN
```

```
      END
      SUBROUTINE FITGAUSS(NO,COEF,NVP,X,N)
*
*    FIT THE LOG OF THE CONCENTRATION VS. DEPTH TO A POLYNOMIAL
*    THIS ROUTINE IS CALLED FITGAUSS BECAUSE IT PREVIOUSLY ONLY
*    FIT THIS DATA TO A POLYNOMIAL OF ORDER 2
*
      DIMENSION COEF(80),XM(80),X(200)
      REAL NM(80),N(200)
      F1(X)=RNG*EXP(-(((X-RP)/SIG)**2)/2)
      PI=3.141592654
      IF (NVP.GT.80)NVP=80
      DO 10 I=1,NVP
      XM(I)=X(I)
      NM(I)=ALOG(N(I))
10    CONTINUE
      CALL FITPOLY(NO,NVP,XM,NM,COEF)
      A=COEF(3)
      B=COEF(2)
      C=COEF(1)
      SIG=SQRT(-1./(2*A))
      RP=-B/2./A
      DOSE=(EXP((C-A*RP**2))*SIG*(2*PI)**.5)/10000.
      RNG=DOSE*10000/SIG/2.5066283
      RETURN
      END
      SUBROUTINE FITPOLY(N,M,X,Y,AA)
*
*     FITS DATA X,Y TO A POLYNOMIAL CURVE
*
      DIMENSION AA(80),A(80,80),X(80),Y(80),XSUM(160),YSUM(160)
*
*    N ---- ORDER OF FIT
*    M ---- NUMBER OF POINTS
      DO 200 I=1,2*N
      XSUM(I)=0
      DO 100 J=1,M
      XSUM(I)=XSUM(I)+X(J)**I
100   CONTINUE
200   CONTINUE
      DO 400 I=0,N
      YSUM(I+1)=0
```

```
          DO 300 J=1,M
          YSUM(I+1)=YSUM(I+1)+(X(J)**I)*Y(J)
300       CONTINUE
400       CONTINUE
          DO 600 I=2,N+1
          DO 500 J=1,N+1
          A(I,J)=XSUM(J+I-2)
500       CONTINUE
600       CONTINUE
          A(1,1)=M
          DO 700 J=1,N
          A(1,J+1)=XSUM(J)
700       CONTINUE
          DO 720 I=1,N+1
          DO 710 J=1,N+1
710       CONTINUE
720       CONTINUE
          CALL SLINEQ(A,N+1,80,AA,YSUM)
          DO 800 I=1,N+1
800       CONTINUE
          RETURN
          END
          SUBROUTINE SLINEQ(A,M,MM,X,Y)
          DIMENSION A(MM,MM),X(MM),Y(MM)
          DIMENSION B(80)
          REAL LU(80,80)
*
*     THE MATRIX LU IS THE LOWER AND UPPER DECOMPOSITION OF THE
*     A MATRIX.  THE DIAGONAL OF THE LU MATRIX BELONGS TO THE LOWER
*     TRIANGULAR MATRIX.  THEREFORE, MULTIPLYING THE ELEMENTS OF THE
*     LU MATRIX DIAGONAL GIVES THE DETERMINANT OF THE A MATRIX.
*
          DET=1
          DO 50 J=1,M
          IF (A(J,J).NE.0) GO TO 50            ! CHECKING FOR ZEROS IN
          DO 75 K=1,M                          ! THE A MATRIX DIAGONAL
          IF (A(K,J).NE.0.AND.A(J,K).NE.0) THEN! IS IT OK TO SWAP ROWS?
          DO 60 L=1,M                          !
          B(L)=A(J,L)                          !
60        CONTINUE                             !
          B(M+1)=Y(J)                          !
          DO 62 L=1,M                          !
```

```
            A(J,L)=A(K,L)                          ! SWAPPING ROWS
62          CONTINUE                               !
            Y(J)=Y(K)                              !
            DO 64 L=1,M                            !
            A(K,L)=B(L)                            !
64          CONTINUE                               !
            Y(K)=B(M+1)                            !
            DET=-1*DET                             !
            GOTO 50
            ENDIF
75          CONTINUE
50          CONTINUE
*
*       BEGIN DECOMPOSING A INTO THE LU MATRIX
*
*
            DO 200 L=1,M                  ! L IS THE MASTER INDEX
            J=L                           ! FIRST DO A COLUMN
            DO 100 I=L,M
            SUM=0
            DO 90 K=1,J-1
            SUM=SUM+LU(I,K)*LU(K,J)
90          CONTINUE
            LU(I,J)=A(I,J)-SUM
100         CONTINUE
            I=L                           ! NOW DO A ROW
            DO 180 J=I+1,M
            SUM=0
            DO 170 K=1,I-1
            SUM=SUM+LU(I,K)*LU(K,J)
170         CONTINUE
            LU(I,J)=(A(I,J)-SUM)/LU(I,I)
180         CONTINUE
200         CONTINUE                  ! DO ANOTHER COLUMN AND ROW
            DO 300 J=1,M              ! NOW CALCULATE THE DETERMINANT
            DET=DET*LU(J,J)
300         CONTINUE
*
*
*       NOW SOLVE THE LINEAR EQUATIONS  (LU)X=Y
*       FIRST TAKE UX=L(-1)Y=B
*       THEN, USING BACK SUBSTITUTION, DETERMINE X
```

```
*
          DO 500 I=1,M              !
          SUM=0                     ! FIRST DETERMINE B BY
          DO 400 K=1,I-1            ! FORWARD SUBSTITUTION
          SUM=SUM+LU(I,K)*B(K)      !
400       CONTINUE                  !        LB=Y
          B(I)=(Y(I)-SUM)/LU(I,I)   !
500       CONTINUE                  !----------------------
          DO 700 I=M,1,-1           ! NOW DETERMINE X BY
          SUM=0                     ! BACK SUBSTITUTION
          DO 600 K=I+1,M            !
          SUM=SUM+LU(I,K)*X(K)      !         UX=B
600       CONTINUE                  !
          X(I)=B(I)-SUM             !
700       CONTINUE                  !
          RETURN
          END
          SUBROUTINE NMEAS(DOSE,RP,SIG,H0,NVP,W,X,N)
*
*     THIS PROGRAM FINDS THE MEASURED PROFILE FROM A KNOWN PROFILE.
*     THE DEPLETION WIDTHS ARE IN THE FILE 'DEPW.DAT' AND THE MEASURED
*     PROFILE IS OUTPUT TO THE FILE 'NMEAS.DAT'
*
*
          DIMENSION W(0:200),XS(0:200),X(200)
          REAL N(200)
          FNN(X)=RNG*EXP(-(((X-RP)/SIG)**2)/2)
          DO 10 I=0,NVP
          XS(I)=I*H0
10        CONTINUE
          RNG=DOSE*10000/SIG/2.5066283
          NINT=5000
          OPEN(UNIT=12,STATUS='NEW',FILE='NMEAS.DAT')
          WRITE(12,*)NVP,2
          DO 100 I=0,NVP-1
          SUM=0
          DX=(XS(I+1)-XS(I)+W(I+1)-W(I))/NINT
          DO 20 Y=XS(I)+W(I),XS(I+1)+W(I+1),DX
          SUM=SUM+FNN(Y)
20        CONTINUE
          X(I+1)=(XS(I)+XS(I+1))/2
          N(I+1)=SUM*DX/H0
```

```
            WRITE(12,*)X(I+1),N(I+1)
100         CONTINUE
            CLOSE(12)
            RETURN
            END
```

Bibliography

1. Dearnaley, G. et al. Ion implantation. Amsterdam: North-Holland Publishing Company, 1973.
2. Morgan, D.V. et al. "Prospects for Ion Bombardment and Ion plantation in GaAs and InP Device Fabrication," IEE Proceedings, 128: 109-130, August 1981.
3. Stephens, K.G. and Sealy, B.J. "Use of ion implantation in future GaAs technology," Microelectronics, J.9: 13-18, 1978.
4. Yeo, Y.K. et al. "Surface-depletion effect correction to nonuniform carrier distributions by Hall measurements," Journal of Applied Physics, 61 (11): 5070-5075, june 1987.
5. Gibbons, J.F. et al. "Projected Range Statistics: Semiconductors and Related Materials," Dowden, Hutchinson and Ross, Inc., 1975.
6. Carter, G. and Grant, W.A. "Ion Implantation of Semiconductors," Chap. 3, Edward Arnold, Ltd., London, 1976.
7. Chandra, A. et al. "Surface and Interface Depletion Corrections to Free Carrier Density Determinations by Hall Measurements," Solid State Electronics, 22, pp 645-650, December 1979.
8. Many, A. et al. Semiconductor Surfaces. Amsterdam: North-Holland Publishing Company, 1965.
9. Bardeen, J. "Surface States and Rectification at a Metal Semiconductor Contact," Physical Review, 71, pp 717-727, 1947.
10. Mckelvey, J.P. Solid State and Semiconductor Physics. Malabar, Fla.: Robert & Krieger Publishing Co., 1966.
11. Shockley, W. "On the surface states associated with a periodic potential," Physical Review, 56, 317-323, August 1939.
12. Massies, J. et al. "Application of Molecular Beam Epitaxy to Study the Surface Properties of III-V Compounds," Proceedings of the 3rd International Conference on Solid Surfaces, pp 639-646, Vienna, 1977.
13. Henisch, H.K. Rectifying Semiconductor Contacts. Oxford: The Clarendon Press, 1957.
14. Schottky, W. "Verinfachte und Erweiterte Theorie der Randschichtgleichricter," Zeitchrift fur Physik, 118, pp 539-592, September 1942.

15. Copeland, J.A. "A technique for Directly Plotting the Inverse Dopping Profile of Semiconductor Wafers," IEEE Transactions on Electron Devices, ED 16, No 5, pp 445-449, May 1969.

16. Miller, L. "A Feedback Method for Investigating Carrier Distributions in Semiconductors," IEEE Transactions on Electron Devices, ED 19, No 10, pp 1103-1198, October 1982.

17. Nakhamanson, R.S. "A Technique for Directly Plotting the Doping Profile of Semiconductor Wafers ('8-Shaped Way')," Solid State Electronics, 19, pp 84-89, 1976.

18. Kim, Y.Y. Electrical Properties of Silicon-Inplanted GaAs. MS Thesis. PH-82d-17. School of Engineering, Air Force Institute of Technology (AU), Wright-Patterson AFB, OH, December 1982.

19. Giacoletto, L. "Junction Capacitance and Related Characteristics Using Graded Impurity Semiconductors," IRE Transactions on Electron Devices, ED 4, pp 207-215, July 1957.

20. Sze, S.M. Physics of Semiconductor Devices, (2nd Ed.). Murray Hill, New Jersey: John Wiley & Sons, 1981.

21. Wu, C.P. et al. "Limitations of the CV technique for Ion-Implanted Profiles," IEEE Transactions on Electron Devices, ED 22, No 6, pp 319-329, June 1975.

22. Norwood, H.M. et al. "Voltage Variable Capacitor Tuning: A Review," Proceedings of the IEEE, Vol 56, No 5, pp 788-798, May 1968.

23. Klopfenstein, R.W. and Wu, C.P. "Computer Solution of One-Dimensional Poisson's Equation," IEEE Transactions on Electron Devices, ED 22, No 6, pp 329-333, June 1975.

24. NASA. Charaterization of Silicon-Gate CMOS/SOS Integrated Circuits with Ion Implantation. Brief no. MFS-23995. Marshal Space Flight Center, 1977.

25. van der Pauw, L.J. "A Method of Measuring specific Resistivity and Hall-Effect of Discs of Arbitrary Shape." Phillips Research Reports, 13: 1-9, February 1958.

26. Moline, R.A. "Ion-Implanted *Phosphorus in Silicon* : Profiles using C-V Analysis," J. Appl. phys. , vol. 42, p. 3553, 1971.

27. Seidel, T.E. "Distribution of Boron-Implanted Silicon," Proc. 2nd Int. Conf. Ion Implantation in Semiconductors, vol. 2, pp. 1-47, May 1971.

28. Reddi, V.G.K. and Yu, A.Y.C. "Ion implantation for Silicon Device Fabrication," Solid State Technol. , p.35, Oct. 1972.

29. Zohta, Y. "Rapid Determination of Semiconductor Doping Profiles in MOS Structures," Solid State Electronic, vol. 16, p. 124, 1972.

30. Lindhard, J. ,Scharff, M. and Schoitt, H.K. "Range Concepts and Heavy Ion Ranges," Kgl. Dan. Vidensk. Selsk. , Mat. Fys. Medd., vol. 33, p. 39, 1963.

31. Kennedy, D.P. and O'Brien, R.R. "On the Measurement of Impurity Atom Distributions by the Differential Capacitance Technique," IBM J. Res. Develop. , vol. 13, p.212, 1969.

32. Gainer, G.H. Calculation Depletion Region Carrier Concentrations with C-V Measurements and Etching. MS Thesis. GEP-87D. School of Engineering, Air Force Institute of Technology (AU), Wright-Patterson AFB, OH, December 1987.

Vita

Jong Hyun Kim [redacted] He graduated from high school in Seoul in 1981 and entered the Korea Military Academy from which he received the degree of Bachelor of Science in Electrical Engineering in March 1985. Upon graduation he was commisioned in the ROKA. He immediately began active duty and served as Platoon Leader in Field Infantry. In May 1987, he entered the School of Engineering, Air force Institute of Technology.

[redacted]